Statistical Hadronization and Quark Chemistry

Andong, HI meeting May 20, 2006

OBJECTIVES:

1. **Energy into matter: (statistical) hadronization of quark-gluon plasma;**
2. **Study the properties of dense fireball at RHIC-200, and HIC as function of $\sqrt{s}$;**
3. **Extend this**
   a) **to LHC: possible range of soft hadron production;**
   b) **dynamical hadronization model – future**

Supported by a grant from the U.S. Department of Energy, DE-FG02-04ER41318

Travel support by the Korean HI group and the Andong University is gratefully acknowledged

Johann Rafelski
Department of Physics
University of Arizona
TUCSON, AZ, USA

CONTENTS

1. Introduction: Riddle of QGP hadronization

Hadronization is the transformation of hot, deconfined quark matter (QGP) into hadrons. The presence of an initial dense nearly chemically equilibrated deconfined fireball is assumed. Depending on the dynamics, the QGP fireball can either:

1. **evaporate and/or break-up into hadronic particles WITHOUT formation of hadron gas (HG) phase or**
2. **the QGP converts into a well defined equilibrating space-time domain filled with hadrons.**

The first case is called sudden hadronization, and yields of final state hadrons are not expected to be in hadron chemical equilibrium, especially so if QGP was chemically equilibrated. In both cases, the individual hadron production is determined by the properties of the accessible phase space, the same in both cases. Analysis seeking to understand hadronization must not constrain the system to be in the hadro-chemical equilibrium.

There is considerable confusion generated by inexperienced (e.g young, experimental) scientists analyzing data. Study of spectra much more difficult as dynamics of expansion influences the shape AND hadronization condition.

NEW (TWO STEP) HADRON FORMATION MECHANISM IN QGP

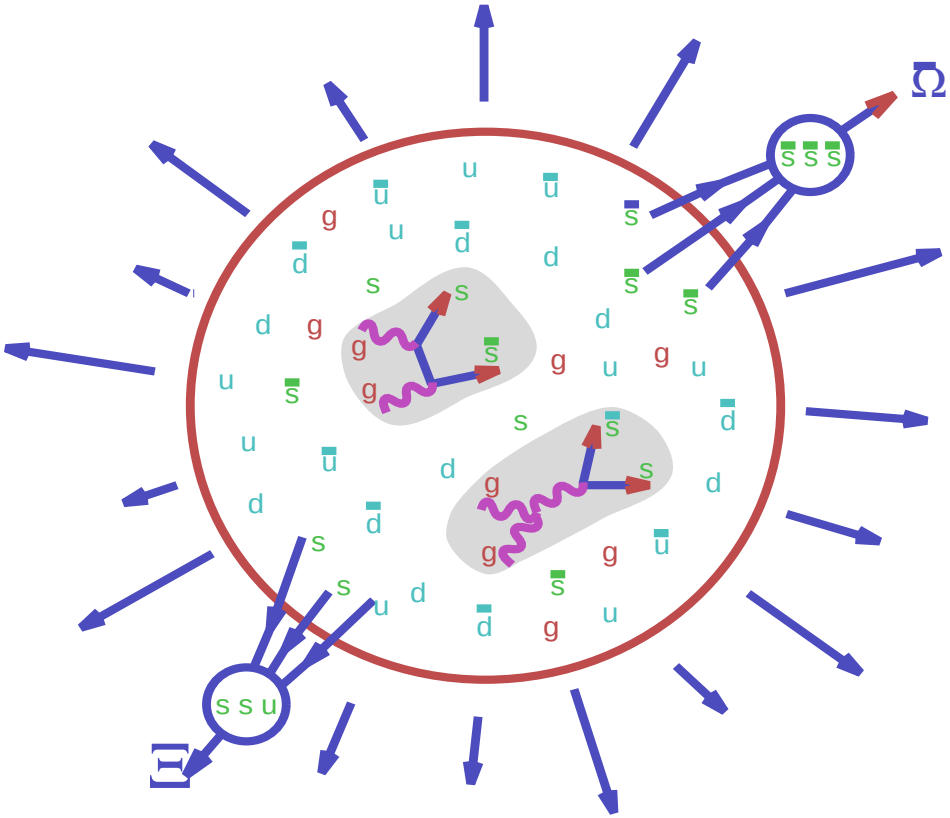

1. **Flavor production in QGP**

   $GG \leftrightarrow q\bar{q}$ **equilibration**

   $GG \rightarrow s\bar{s}$ **(hot thermal gluons collide)**

   $GG \rightarrow c\bar{c}$ **(initial parton collision)**

   gluon dominated reactions

2. **hadronization of pre-formed**

   $q, \bar{q}$ s, $\bar{s}$, c, $\bar{c}$ **quarks**

Mechanism alters meson to baryon ratio, favors the formation of complex rarely produced (multi)exotic flavor (anti)particles from QGP enabled by coalescence between s, $\bar{s}$, c, $\bar{c}$ quarks made in different microscopic reactions; this is signature of quark mobility and independent action, thus of deconfinement. Enhancement of flavored (strange, charm) antibaryons progressing with 'exotic' flavor content.

AVAILABLE CONFIRM:

Big change in relative baryon to meson yields, and common new mechanism of matter-antimatter formation, enhancement of strange (anti)baryons which progresses with strangeness content. See: P. Koch, B. Muller and J. Rafelski, *Strangeness In Relativistic Heavy Ion Collisions,* **Phys. Rept. 142, 167 (1986), and references therein.**

Baryon to Meson Ratio

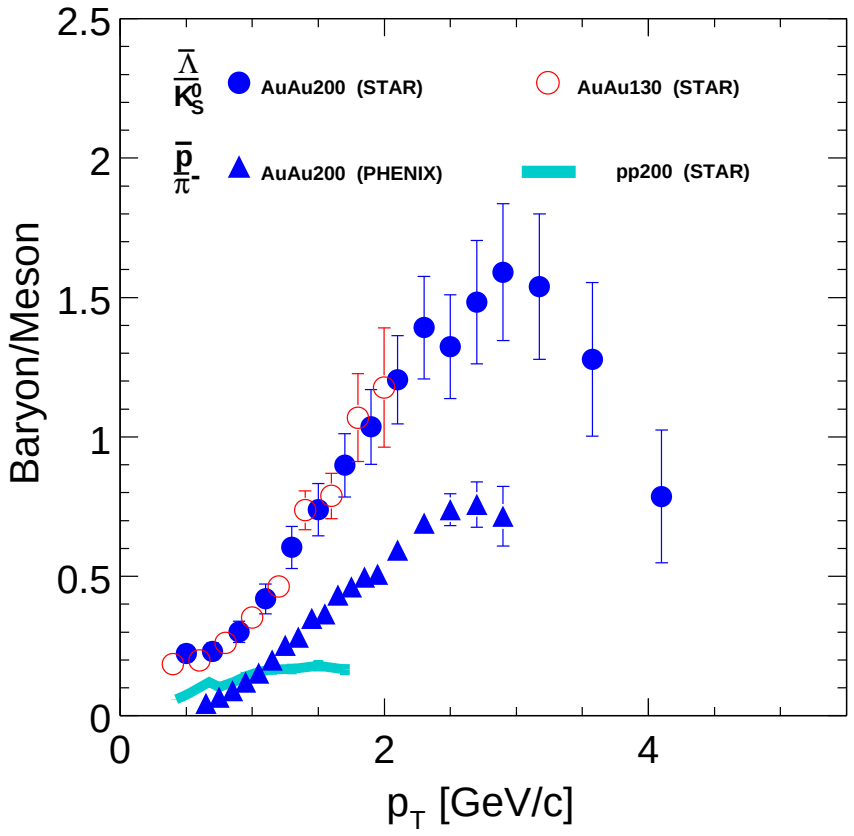

EXAMPLE: Ratios of $\overline{\Lambda}$ to K_S from AuAu and pp collisions (STAR) and $\overline{p}$ to π from AuAu collisions (PHENIX) as a function of transverse momentum ($p_\perp$). The large ratio at the intermediate $p_\perp$ region provide clear evidence that particle formation dynamics in AA collisions at RHIC are distinctly different from the traditional hadron formation mechanism via STRING fragmentation processes developed for the elementary e^+e^- and nucleon-nucleon collisions, see here STAR pp results.

SYMMETRIC MATTER-ANTIMATTER PRODUCTION

For the past 15 years experiments demonstrate symmetry of $m_\perp$ spectra of strange baryons and antibaryons in baryon rich environment.

Interpretation: Common matter-antimatter particle formation mechanism, little antibaryon re-annihilation in sequel evolution.

Appears to be free-streaming particle emission by a quark source into vacuum. Such fast hadronization confirmed by other observables: e.g. reconstructed yield of hadron resonances. Note: within HBT particle correlation analysis: nearly same size pion source at all energies

Practically no hadronic 'phase'!
No 'mixed phase' either!
Direct emission of free-streaming hadrons from exploding filamentary QGP

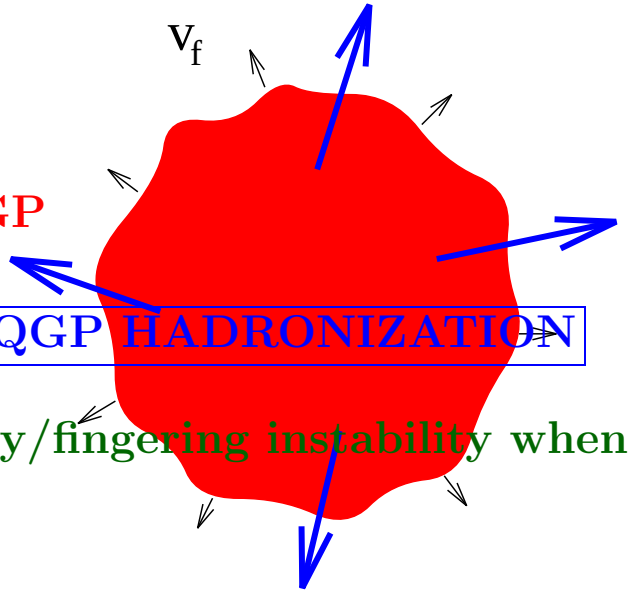

Develop analysis tools viable in SUDDEN QGP HADRONIZATION

Proposed reaction mechanism: filamentary/fingering instability when in expansion pressure reverses.

WA97	$T_\perp^{\rm Pb}$ **[MeV]**
T^{Λ}	**289 ± 3**
$T^{\overline{\Lambda}}$	**287 ± 4**
T^{Ξ}	**286 ± 9**
$T^{\overline{\Xi}}$	**284 ± 17**
$T^{\Omega+\overline{\Omega}}$	**251 ± 19**

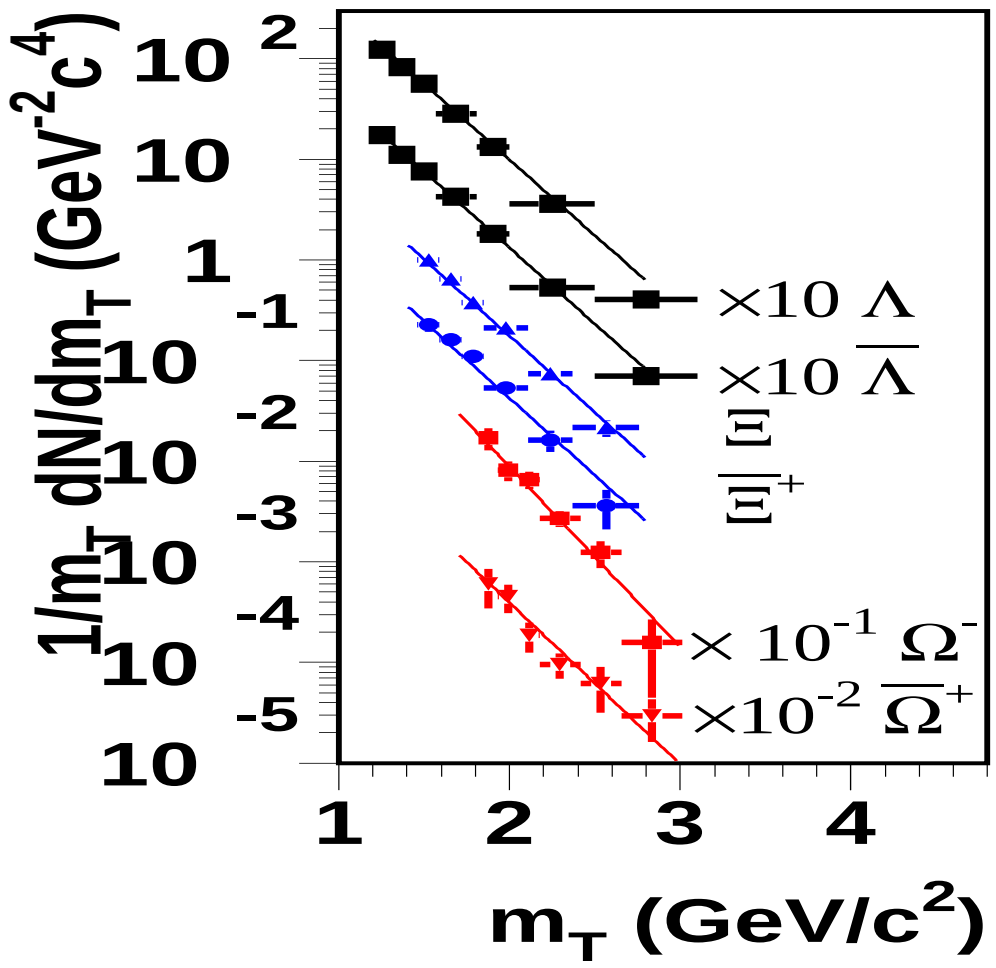

T_Λ **within 1% of** $T_{\overline{\Lambda}}$

CERN-WA97 result

$\Xi^-, \overline{\Xi^-}$ Spectra RHIC-STAR 130+130 A GeV

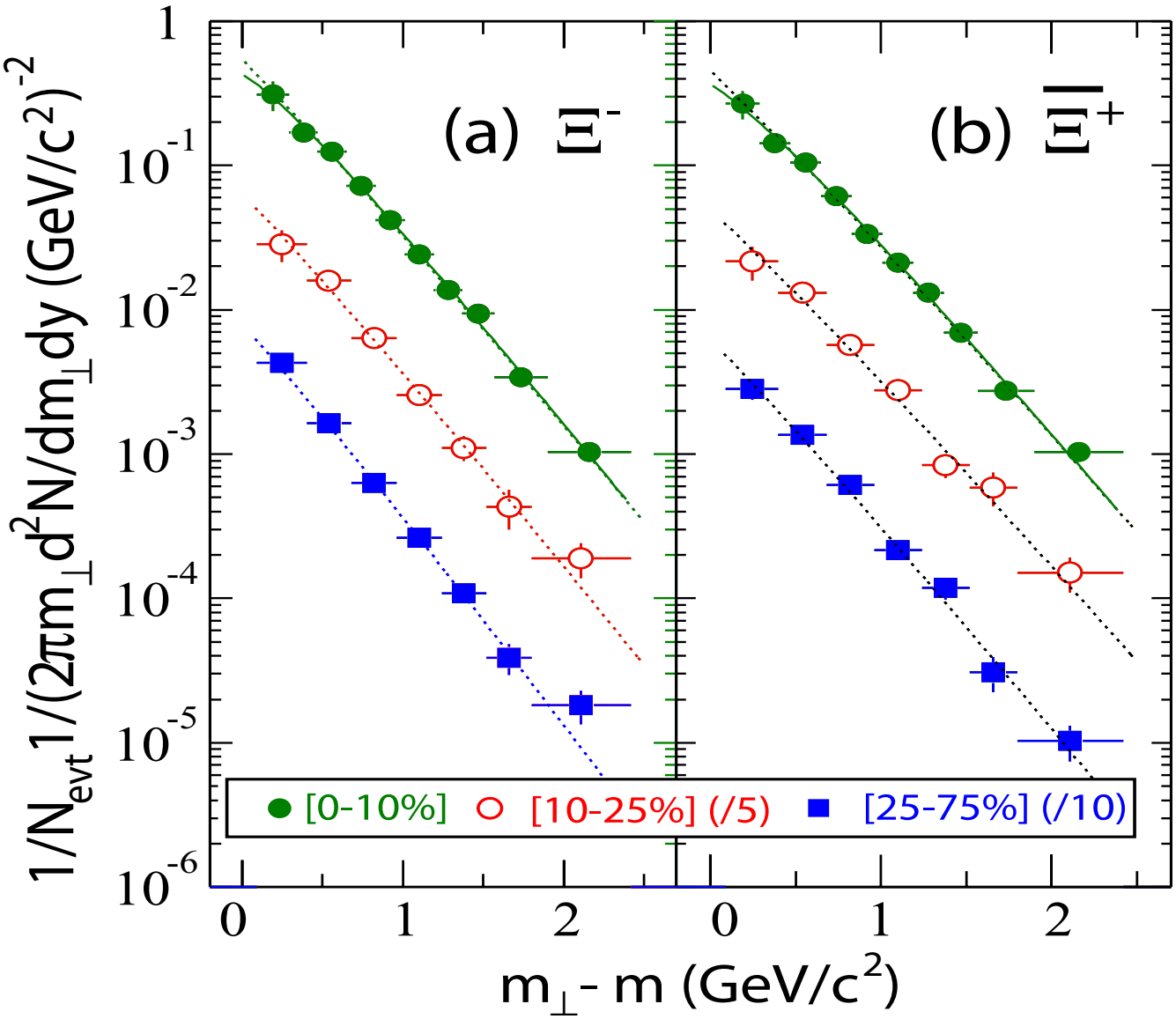

YIELD ENHANCEMENT AS FUNCTION OF CENTRALITY

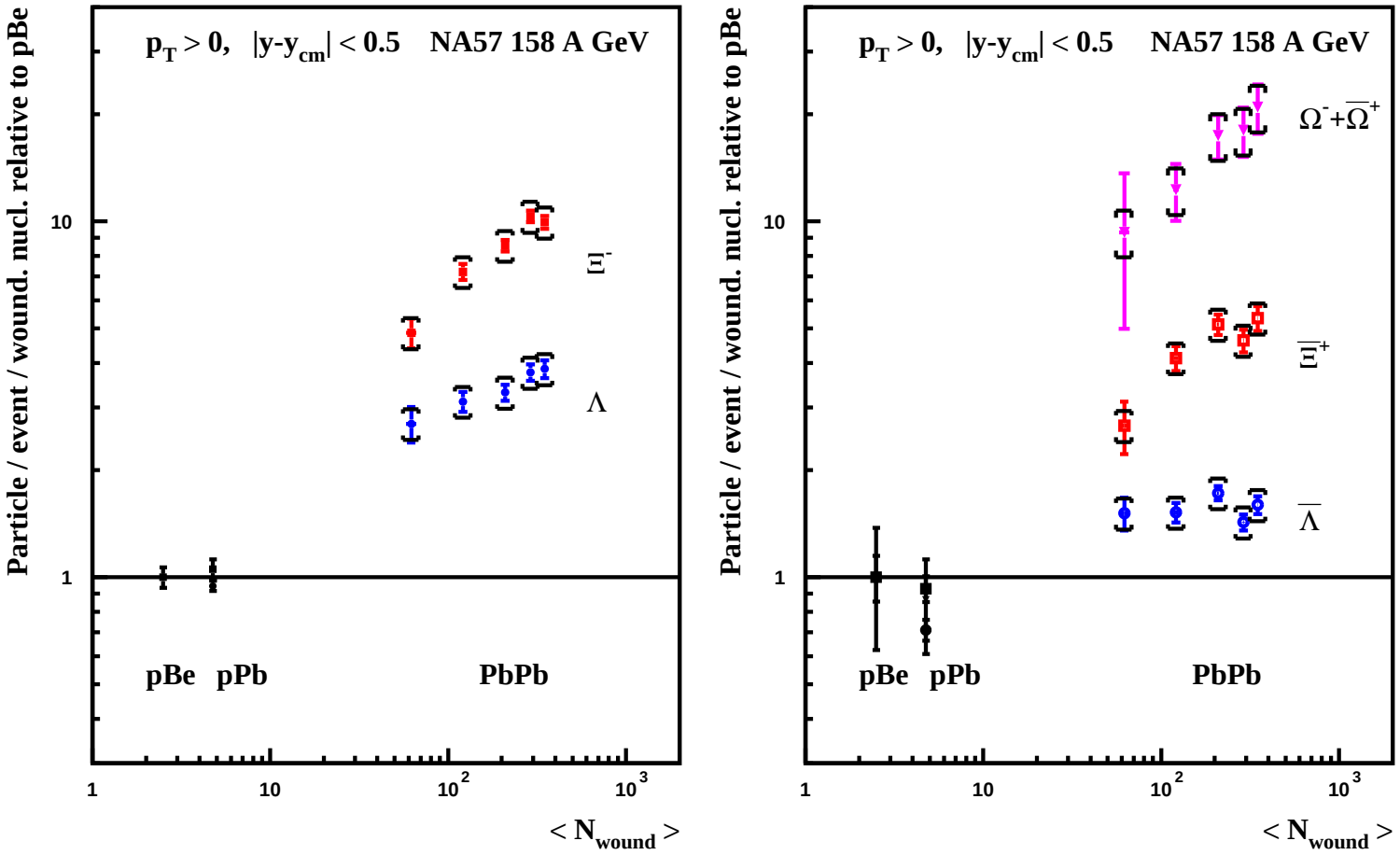

Note the gradual onset of enhancement with reaction volume.
Alternate models e.g. "canonical enhancement" (a hadronic equilibrium model) is grossly inconsistent with this, as it is inconsistent with energy dependence.
Gradual enhancement shown predicted by study of kinetic strangeness production (Seoul seminar).

2. Tutorials – Relativistic Statistical Method

The distribution $n = \{n_i\}$ of $N = \sum n_i$ elements having the same energy $E^{(N)} = \sum n_i E_i$ can be achieved in many different ways. To find how many, consider:

$$K^N = (x_1 + x_2 + \cdots + \cdots x_K)^N|_{x_i=1} = \sum_n \frac{N!}{n_1! n_2! \cdots n_K!} x_1^{n_1} x_2^{n_2} \cdots x_K^{n_K}|_{x_i=1}.$$

The normalized coefficients are the relative probabilities of realizing each state in the ensemble n, with n_i equivalent elements. To find the most probable distribution $\overline{n}$ subject to the constraints of fixed total particle number and energy we introduce two Lagrange multipliers a and β and look for an extremum of:

$$A(n_1, n_2, \ldots, n_K) = \ln W(n) + \ln\gamma \sum_i n_i - \beta \sum_i n_i E_i,$$

$$\frac{\partial}{\partial n_i}[-\ln(n_i!) + \ln\gamma n_i - \beta n_i E_i]\Big|_{\bar{n}_m} = 0. \qquad \frac{d}{dk}[\ln(k!)] \approx \frac{\ln(k!) - \ln[(k-1)!]}{(k) - (k-1)} = \ln k.$$

We find the most probable distribution: $\bar{n}_i = \gamma e^{-\beta E_i}$, the inverse of the slope parameter β can be shown to be temperature.
The particle number $\sum_i \bar{n}_i = \gamma \sum_{i=1}^K e^{-\beta E_i} = N$ is fixed by the chemical fugacity γ.
The energy $E^{(N)} = \sum_i \bar{n}_i E_i = \gamma \sum_i E_i e^{-\beta E_i}$. divided by N,

$$\frac{E^{(N)}}{N} \equiv \overline{E^{(N)}} = \frac{\gamma \sum_i E_i\, e^{-\beta E_i}}{\gamma \sum_i e^{-\beta E_i}} \equiv -\frac{d}{d\beta} \ln Z; \qquad Z = \sum_i \gamma e^{-\beta E_i}.$$

motivates the introduction of the partition function Z. $\beta = 1/T$

Statistical and thermal physics relations

$$\beta P = \frac{\partial \ln \mathcal{Z}(V,\beta,\mu)}{\partial V}, \qquad E = -\frac{\partial \ln \mathcal{Z}(V,\beta,\mu)}{\partial \beta},$$

$$\mathcal{F}(V,T,\mu) \equiv E(S,b) - ST - \mu b = -P(T,\mu)V,$$

$$S = -\frac{d}{dT}\mathcal{F}(V,T,\mu) = \frac{d}{dT} T \ln \tilde{\mathcal{Z}}(V,T,\mu) = \left.\frac{dP}{dT}\right|_{\mu}$$

Statistical physics Gibbs–Duham relation

$$P = T\sigma + \mu\nu - \epsilon, \quad \sigma = \frac{S}{V}, \quad \nu = \frac{b}{V}, \quad \epsilon = \frac{E}{V},$$

is more powerful than the 1st law of thermodynamics:

$$dE(V,S,b) = -P\,dV + T\,dS + \mu\,db, \qquad d\mathcal{F} = -P\,dV - S\,dT - b\,d\mu,$$

compare to:

$$\epsilon\,dV = -P dV + T\sigma\,dV + \mu\,\nu\,dV$$

Chemical Potentials Tutorial

Particle fugacity: $\Upsilon_i \equiv e^{\sigma_i/T} \Longleftrightarrow \sigma_i$ **particle 'i' chemical potential**

Phase space density is:

$$\frac{d^6N_i}{d^3pd^3x} = g_i\frac{\Upsilon_i}{(2\pi)^3}e^{-E_i/T}, \qquad \frac{d^6N_i^{\rm F/B}}{d^3pd^3x} = \frac{g_i}{(2\pi)^3}\frac{1}{\Upsilon_i^{-1}e^{E_i/T}\pm 1}, \qquad \Upsilon_i^{\rm B} \leq e^{m_i/T},$$

each hadron comprise two chemical factors associated with the two different chemical equilibriums, example of NUCLEONS:

$$\Upsilon_N = \gamma_N e^{\mu_b/T}, \qquad \Upsilon_{\overline{N}} = \gamma_N e^{-\mu_b/T};$$

$$\sigma_N \equiv \mu_b + T\ln\gamma_N, \qquad \sigma_{\overline{N}} \equiv -\mu_b + T\ln\gamma_N.$$

γ determines the number of nucleon-antinucleon pairs,
$\gamma_i(t)$ rises from 0 (initially absent) to 1 for chemical equilibrium.
The (baryo)chemical potential μ_b, controls the particle difference = baryon number.

This can be seen looking at the first law of thermodynamics:

$$dE + P\,dV - T\,dS = \sigma_N\,dN + \sigma_{\overline{N}}\,d\overline{N}$$
$$= \mu_b(dN - d\overline{N}) + T\ln\gamma_N(dN + d\overline{N}).$$

To characterize a particle we follow the valance quark content of a hadron forming a product of factors $\gamma_{u,d,s}$, and $\lambda_{u,d,s}$, e.g. for $p(uud)$:

$$\Upsilon_p = \gamma_u^2\gamma_d\,\lambda_u^2\lambda_d, \qquad \Upsilon_{\bar{p}} = \gamma_u^2\gamma_d\,\lambda_u^{-2}\lambda_d^{-1},$$

note that:

$$\lambda_{u,d,s} = e^{\mu_{u,d,s}/T}, \qquad \mu_q = \frac{1}{2}(\mu_u + \mu_d), \quad \lambda_q^2 = \lambda_u\lambda_d \quad \lambda_b = \lambda_q^3.$$

This implies relations between quark and hadron potential:

$$\mu_b = 3\mu_q \qquad \mu_s = \frac{1}{3}\mu_b - \mu_{\rm S}, \qquad \lambda_s = \frac{\lambda_q}{\lambda_{\rm S}},$$

Note above: NEGATIVE strangeness in s-hadrons, e.g. for $\Lambda(uds)$:

$$\Upsilon_\Lambda = \gamma_u\gamma_d\gamma_s\,e^{\mu_u+\mu_d+\mu_s}, \qquad \Upsilon_{\overline{\Lambda}} = \gamma_u\gamma_d\gamma_s\,e^{-\mu_u-\mu_d-\mu_s},$$

CHEMICAL (NON)EQUILIBRIUM:

γ_i controls overall abundance of quark 'i' pairs	Absolute chemical equilibrium
λ_i controls difference between strange and non-strange quarks 'i'	Relative chemical equilibrium

EXAMPLE: Strangeness in HG:
Relative chemical equilibrium Absolute chemical equilibrium

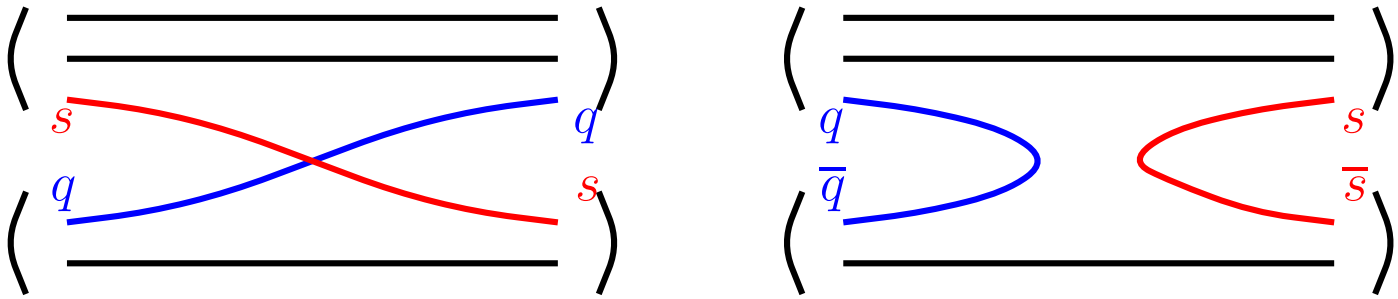

EXCHANGE REACTION **PRODUCTION REACTION**

Absolute equilibrium $\gamma \to 1$ require more rarely occurring truly inelastic collisions with creation of new particles.

Equilibrium – Phase Transition Tutorial

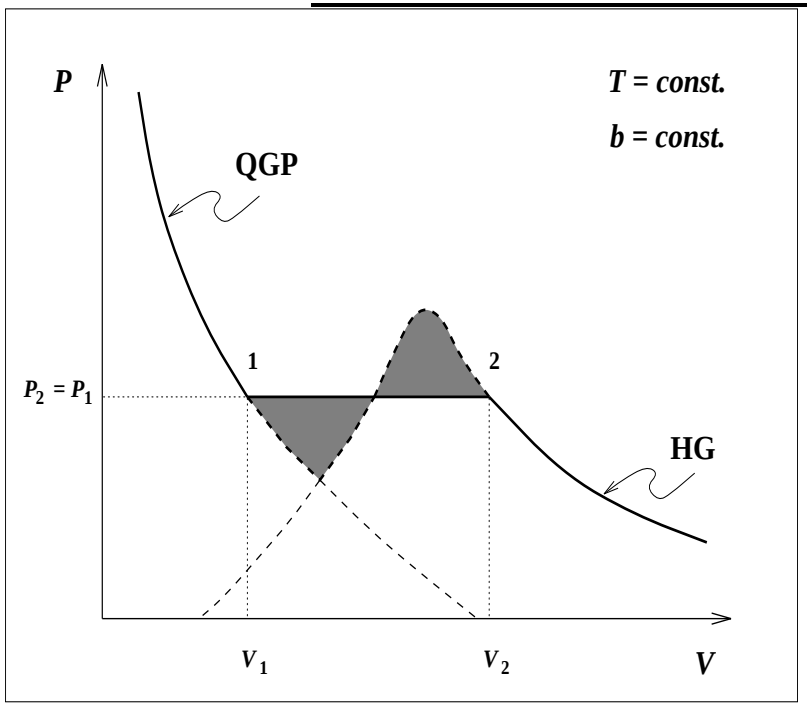

The P–V diagram for the QGP–HG system, shown at fixed temperature and baryon number; dashed lines indicate unstable domains of overheated and undercooled phases. Darkened area: Maxwell construction, connecting the volumes $V_1 = b/\rho_1$ and $V_2 = b/\rho_2$, such that work done along the metastable branches vanishes:

$$\int_{V_1}^{V_2} (P - P_{12})\, dV = 0.$$

Construction can be repeated for different values of b and T, the set of resulting points 1 and 2 forms then two phase-boundary lines.

Between V_1 and V_2 is the mixed phase comprising a mixture of hadrons and drops of QGP. Such a phase formed in early Universe but probably NOT in laboratory experiments.

In a second order phase transition, a discontinuity in e.g. energy density or baryon density is not present, higher order derivatives of partition function are discontinuous.

Relativistic gas tutorial

$$\ln \mathcal{Z}_{\rm F/B}(V,\beta,\lambda,\gamma) = \pm gV \int \frac{d^3p}{(2\pi)^3}\,[\ln(1\pm\gamma\lambda e^{-\beta\sqrt{p^2+m^2}}) + \ln(1\pm\gamma\lambda^{-1}e^{-\beta\sqrt{p^2+m^2}})];$$

Boltzmann limit:

$$\ln \mathcal{Z}_{\rm cl}(V,\beta,\lambda,\gamma) = gV \int \frac{d^3p}{(2\pi)^3}\,\gamma(\lambda+\lambda^{-1})e^{-\beta\sqrt{p^2+m^2}}.$$ **for Fermi and Bose**

– a useful integral –

$$W(\beta m) \equiv \beta^3 \int e^{-\beta\varepsilon} p^2\, dp = (\beta m)^2 K_2(\beta m), \quad \to 2, \ \textbf{for } m\to 0, \quad \to \sqrt{\frac{\pi m^3}{2T^3}} e^{-m/T}, \ \textbf{for } m \gg T$$

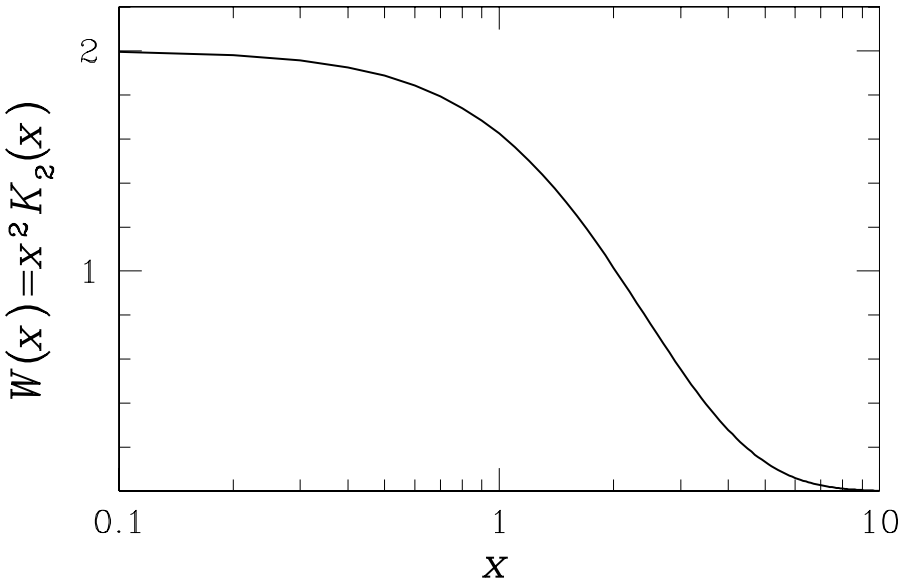

$$\ln \mathcal{Z}_{\rm cl} \equiv Z^{(1)} = \sum_i \gamma_i(\lambda_i+\lambda_i^{-1})Z_i^{(1)},$$

$$Z_i^{(1)} = g_{\rm f} V \int \frac{d^3p}{(2\pi)^3} e^{-\beta\varepsilon(p)}$$

$$= g_i \frac{\beta^{-3}V}{2\pi^2} W(\beta m_i).$$

Sums of W(x)

Relativistic Bose gas, e.g. photon, gluons, pions: exploit the sum:

$$f(\varepsilon) = \frac{1}{\gamma^{-1}e^{\beta\varepsilon} - 1} = \sum_{n=1}^{\infty} \gamma^n e^{-n\beta\varepsilon}, \quad \gamma < e^{\beta m}.$$

or for the partition function

$$\ln \mathcal{Z} = -gV \int \frac{dp^3}{(2\pi)^3} \ln(1 - \gamma e^{-\beta\varepsilon}) = \frac{gV}{2\pi^2} \int_0^{\infty} dp p^2 \sum_{n=1}^{\infty} \frac{\gamma^n}{n} e^{-n\beta\varepsilon}, \quad \gamma < e^{\beta m}.$$

Exchange integral and sum! As we see, each term in the sum differs by $\beta \to n\beta$ and all we have to do it so make sure that we have the right power of $1/n$ in the final expression from substitution. Example: particle density:

$$\rho = \frac{g}{2\pi^2} T^3 \sum_{n=1}^{\infty} \frac{\gamma^n}{n^3} \int_0^{\infty} dx\, x^2 e^{-\sqrt{(nm/T)^2 + x^2}} = \frac{\beta^{-3} g}{2\pi^2} \sum_{n=1}^{\infty} \frac{\gamma^n}{n^3} (n\beta m)^2 K_2(n\beta m) \to \frac{gT^3}{\pi^2} \sum_{n=1}^{\infty} \frac{1}{n^3}.$$

Recall Riemann zeta function:

$$\zeta(k) = \sum_{n=1}^{\infty} \frac{1}{n^k}, \ \zeta(2) = \frac{\pi^2}{6}, \ \zeta(3) \simeq 1.202, \ \zeta(4) = \frac{\pi^4}{90}.$$

For a Fermi occupation function, the signs of the terms in the sums are alternating, which leads to the eta function

$$\eta(k) = \sum_{n=1}^{\infty} (-1)^{n-1} \frac{1}{n^k} = (1 - 2^{1-k})\zeta(k), \ \eta(3) = \frac{3}{4}\zeta(3) = 0.901\,5, \ \eta(4) = \frac{7}{8}\zeta(4) = \frac{7}{720}\pi^4.$$

Hot Hadron Tutorial: Limiting Hagedorn Temperature

A gas of hadrons with exponentially rising mass spectrum:

$$\ln \mathcal{Z}^{\rm cl}_{\rm HG} = cV\left(\frac{T}{2\pi}\right)^{3/2}\int_M^\infty m^a e^{m/T_{\rm H}} m^{3/2} e^{-m/T}\, dm + D(T,M),$$

Cutoff $M > m_a > T_{\rm H}$ is arbitrary, its role is to separate off $D(T,M) < \infty$. Because of the exponential factor, the first integral can be divergent for $T > T_{\rm H}$, and the partition function is singular for $T \to T_{\rm H}$ for a range of a:

$$P(T) \to \begin{cases} \left(\frac{1}{T}-\frac{1}{T_{\rm H}}\right)^{-(a+5/2)}, & \text{for} \quad a > -\frac{5}{2}, \\ \ln\left(\frac{1}{T}-\frac{1}{T_{\rm H}}\right), & \text{for} \quad a = -\frac{5}{2}, \\ \text{constant}, & \text{for} \quad a < -\frac{5}{2}; \end{cases} \qquad \epsilon \to \begin{cases} \left(\frac{1}{T}-\frac{1}{T_{\rm H}}\right)^{-(a+7/2)}, & \text{for} \quad a > -\frac{7}{2}, \\ \ln\left(\frac{1}{T}-\frac{1}{T_{\rm H}}\right), & \text{for} \quad a = -\frac{7}{2}, \\ \text{constant}, & \text{for} \quad a < -\frac{7}{2}. \end{cases}$$

The energy density ϵ goes to infinity for $a \geq -\frac{7}{2}$, when $T \to T_{\rm H}$.

Mass spectrum slope $T_{\rm H}$ appears as the limiting Hagedorn temperature beyond which we cannot heat a system which can have an infinite energy density. The partition function can be singular even when $V < \infty$.

Exponential Hadron Mass Spectrum

RH discovered that the exponential growth of the hadronic mass spectrum could lead to an understanding of the limiting hadron temperature $T_{\rm H} \simeq 160$ MeV,

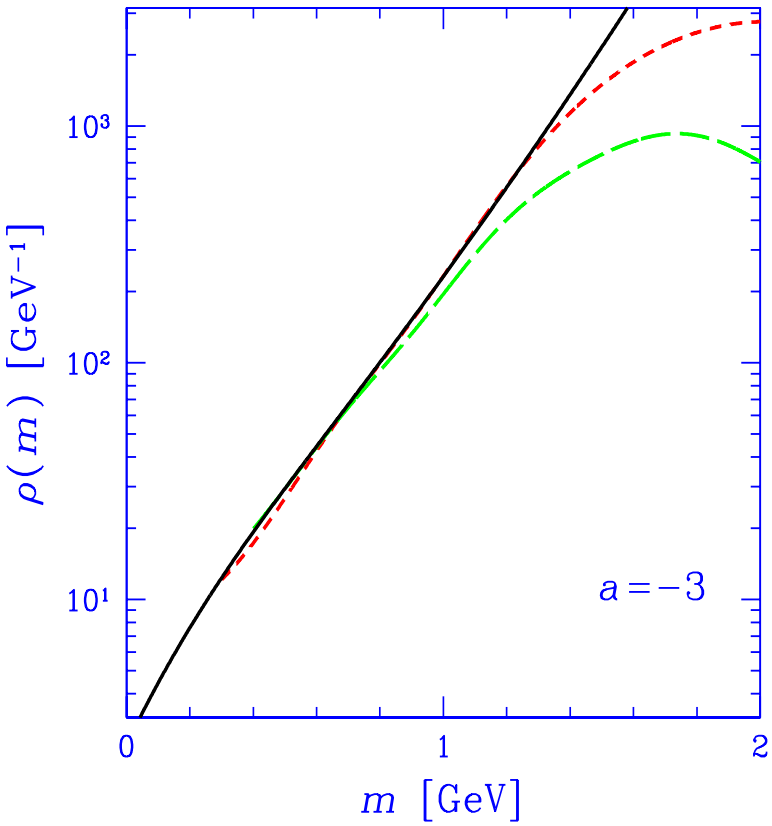

The solid line is the fit:

$$\rho(m) \approx c(m_a^2 + m^2)^{a/2} \exp(m/T_{\rm H})$$

with $a = -3$, $m_a = 0.66$ GeV, $T_{\rm H} = 0.158$ GeV.
Long-dashed line: 1411 states of 1967.
Short-dashed line: 4627 states of 1996.

Experimental lines include Gaussian smoothing:

$$\rho(m) = \sum_{m^*=m_\pi, m_\rho, \ldots} \frac{g_{m^*}}{\sqrt{2\pi}\sigma_{m^*}} \exp\left(-\frac{(m-m^*)^2}{2\sigma_{m^*}^2}\right).$$

$\sigma = \Gamma/2$, $\Gamma = \mathcal{O}(200)$ MeV is the assumed width of the resonance, excluding the 'stable' pion, a special case.

Note the missing resonances at $m > 1.4GeV$.

The 'pentaquark' resonances nicely fill this gap.

Hagedorn Temperature is:

1. **The intrinsic temperature at which hadronic particles are formed, in pp interactions seen as the inverse slope of hadron spectra.**
2. **This boiling point of hadrons which is the (inverse) slope of exponentially rising hadron mass spectrum.**
3. **The boundary value of temperature at which finite size hadrons coalesces into one cluster consisting of a new phase comprising hadron constituents.**

Statistical Bootstrap Model is:

1. **A connection between hadronic particle momentum distribution and properties of hadronic interactions dominated by resonant scattering, and exponentially rising mass spectrum.**
2. **A theoretical framework for study of the properties of the equations of state of dense and hot baryonic matter (nuclear matter at finite temperature).**
3. **It is not a fundamental dynamical theory, in fact SBM is to be motivated today in terms of properties of the fundamental dynamical approach (QCD).**

Finite Volume Hadron Gas Model

The gas of finite size hadrons with exponential mass spectrum has nearly the same properties as a gas of point hadrons with today experimentally observed mass spectrum. That is why 'statistical hadronization works'.

Point hadron gas in free available volume Δ to have the properties of finite size hadron gas in total mean volume $\langle V\rangle$ (RH/JR 1978+)

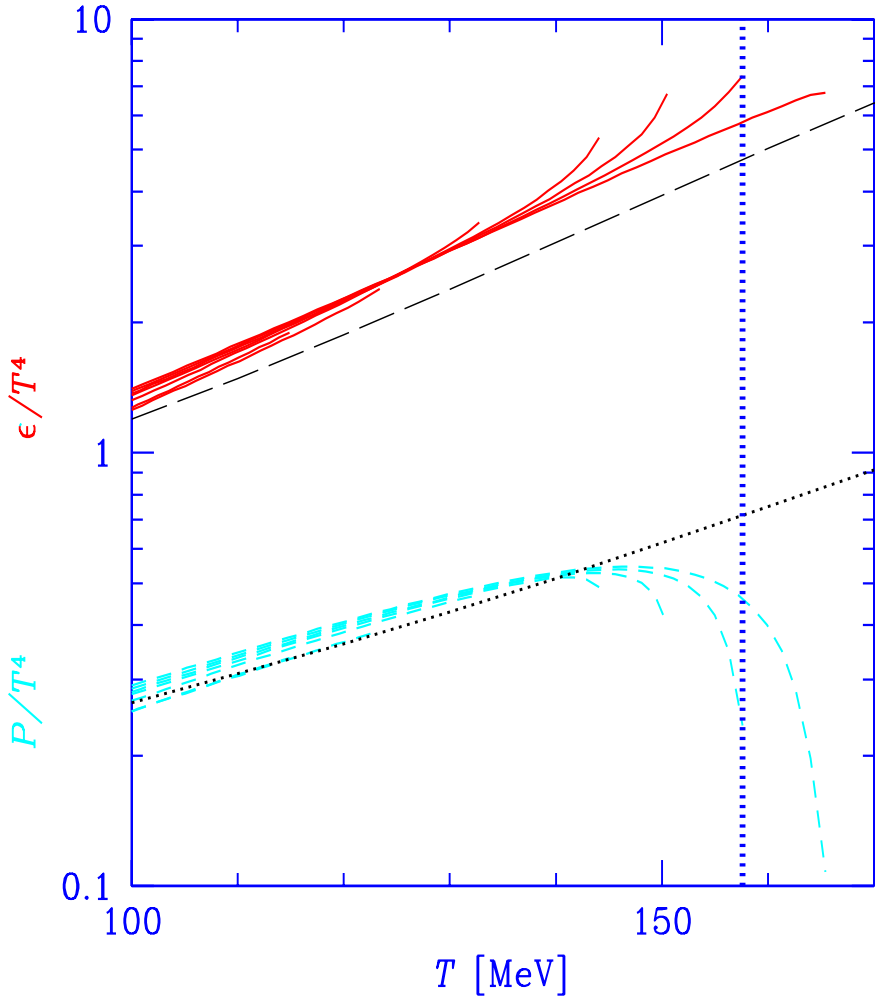

$$\boxed{\ln \mathcal{Z}_{\rm pt}(T,\Delta,\lambda) \equiv \ln \mathcal{Z}(T,\langle V\rangle,\lambda)}$$

Proper particle volume in the rest frame is assumed to be proportional to mass. For a gas of moving hadrons, in gas rest frame: $\langle V\rangle = \Delta + \langle E\rangle/4\mathcal{B}$.

$$\langle E\rangle = \langle V\rangle\epsilon(\beta,\lambda) = -\frac{\partial}{\partial\beta}\ln \mathcal{Z}(\beta,\langle V\rangle,\lambda) =$$

$$= -\frac{\partial}{\partial\beta}\ln \mathcal{Z}_{\rm pt}(\beta,\Delta,\lambda) = \Delta\epsilon_{\rm pt}(\beta,\lambda)$$

$$\langle V\rangle = \Delta\big(1+\epsilon_{\rm pt}(\beta,\lambda)/4\mathcal{B}\big),$$

$$\frac{\langle E\rangle}{\langle V\rangle} \equiv \epsilon(\beta,\lambda) = \frac{\epsilon_{\rm pt}(\beta,\lambda)}{1+\epsilon_{\rm pt}(\beta,\lambda)/(4\mathcal{B})},$$

$$P = \frac{P_{\rm pt}(\beta,\lambda)}{1+\epsilon_{\rm pt}(\beta,\lambda)/4\mathcal{B}}.$$

3. Statistical Hadronization

Hypothesis (Fermi, Hagedorn): particle production can be described by evaluating the accessible phase space. In depth this means that the quantum probability of making a particle is maximized $|\mathcal{M}|^2 \to 1$, so that the accessible phase space only determining factor. When hadrons are evaporated into free-streaming final state there is no re-equilibration of yields. Particle abundances are result of conditions prevailing:

All agree: QGP fireball subject to rapid expansion

REMINDER:

μ_b **controls the particle difference = baryon number.**

γ_i **regulates the number of particle-antiparticle pairs present.**

DISTINGUISH: HG and QGP parameters

Quantities such as baryon number, strangeness, charm, bottom, etc flavors are fixed in hadronization and entropy is almost fixed across any phase boundary, even in presence of a rapid change in STRUCTURE of the phase.

THEREFORE: γ_i **will in general be discontinuous: e.g.** $\gamma_s^{\rm QGP} \neq \gamma_s^{\rm HG}$**. However,** μ_i **are continuous, with the proviso that by definition** $3\mu_q = \mu_{\rm B},\ \mu_s = \mu_{\rm B}/3 - \mu_S$**.**

Physical Impact of Non-Equilibrium Parameters

- $\tilde{\gamma}_s \equiv \gamma_s/\gamma_q$ **shifts the yield of strange vs non-strange hadrons:**

$$\frac{\mathrm{K}^+(u\bar{s})}{\pi^+(u\bar{d})} \propto \frac{\gamma_s}{\gamma_q}\,, \qquad \frac{\phi(s\bar{s})}{h} \propto \frac{\gamma_s^2}{\gamma_q^2}\,, \qquad \frac{\Omega(sss)}{\Lambda(sud)} \propto \frac{\gamma_s^2}{\gamma_q^2}\,,$$

- **For fixed $\tilde{\gamma}_s \equiv \gamma_s/\gamma_q$ and fixed other statistical parameters $(T, \lambda_i, \ldots)$:**

$$\frac{\text{baryons}}{\text{mesons}} \propto \frac{\gamma_q^3}{\gamma_q^2} = \gamma_q\,.$$

Importantly, $\gamma_q > 1$ allows for a significant increase of entropy density. Since QGP is entropy dense state, fast breakup requires that we go from entropy dense phase to another entropy dense phase.

Reminder:Baryon to Meson Ratio

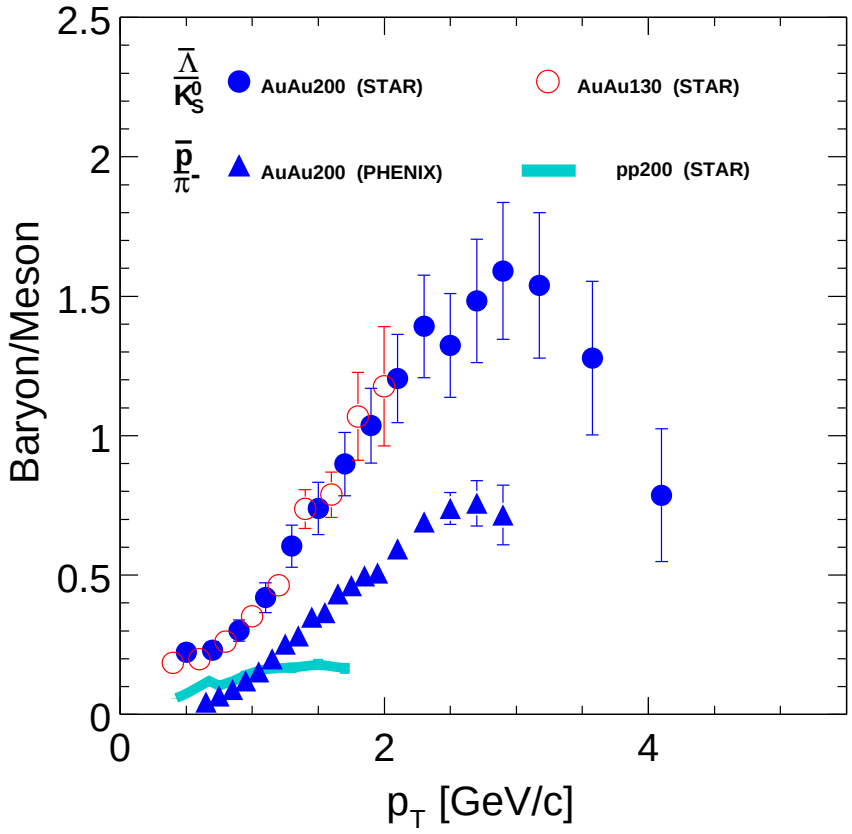

We expect that the value of γ_q depends on system considered with the largest value expected in central A–A at RHIC, and smallest value in p–p, and also low energy AGS A–A reactions. Thus in study of particle yields it is of considerable importance to account for this parameter which remains often ignored.

HIGH ENTROPY STATE AND THE EXPECTED $\gamma_q^{\rm HG}$

QGP has excess of entropy, maximize entropy density at hadronization: $\gamma_q^2 \to e^{m_\pi/T}$:

Example:maximization of entropy density in pion gas $E_\pi = \sqrt{m_\pi^2 + p^2}$

$$S_{\rm B,F} = \int \frac{d^3p\, d^3x}{(2\pi\hbar)^3} \left[\pm(1\pm f)\ln(1\pm f) - f\ln f\right], \qquad f_\pi(E) = \frac{1}{\gamma_q^{-2} e^{E_\pi/T} - 1}.$$

Pion gas properties: N**-particle,** E**-energy,** S**-entropy,** V**-volume as function of** γ_q**.**

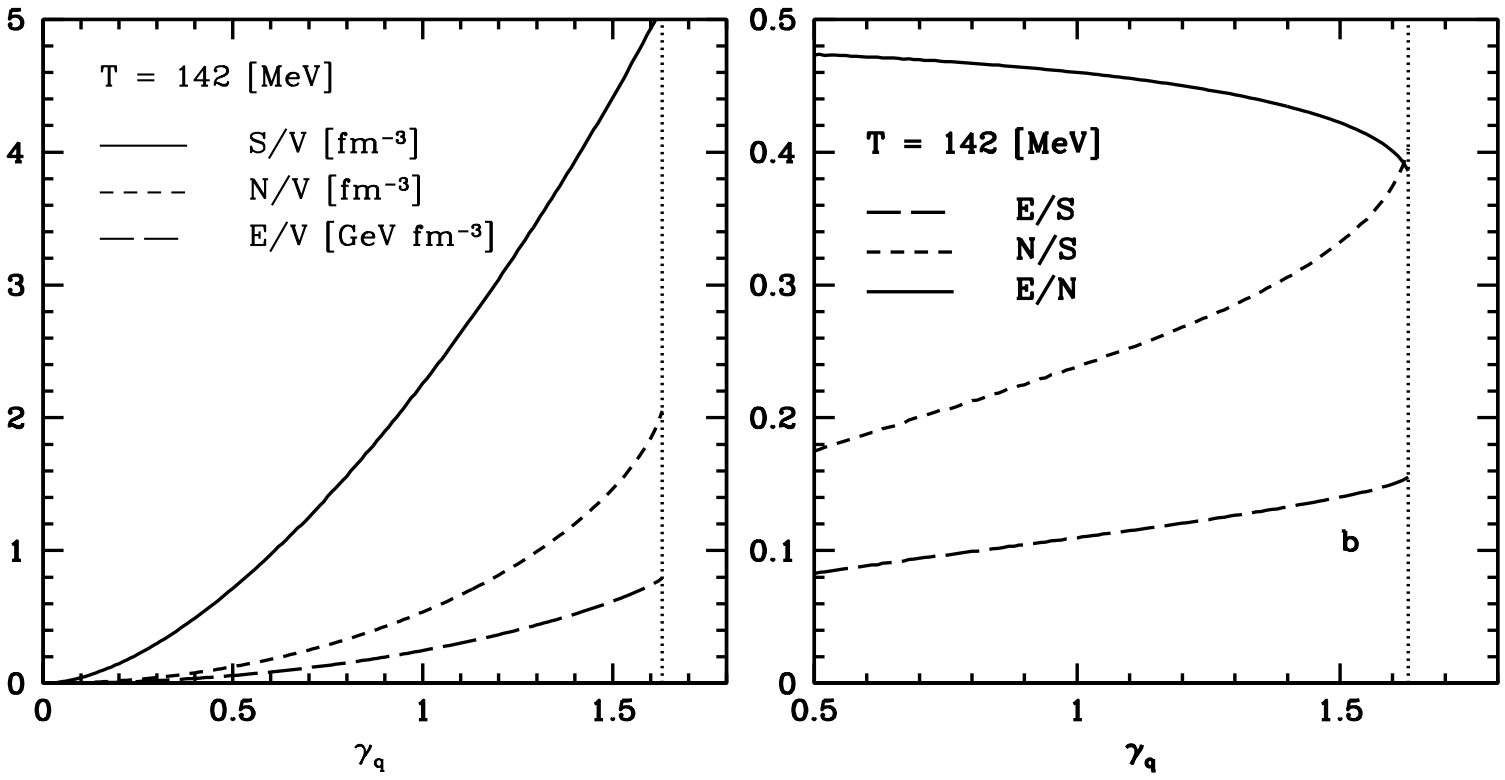

Verification of statistical hadronization:

Particle yields with same valance quark content are in relative chemical equilibrium, e.g. the relative yield of $\Delta(1230)/N$ as of K^*/K, $\Sigma^*(1385)/\Lambda$, etc, is controlled by chemical freeze-out i.e. Hagedorn Temperature $T_{\rm H}$:

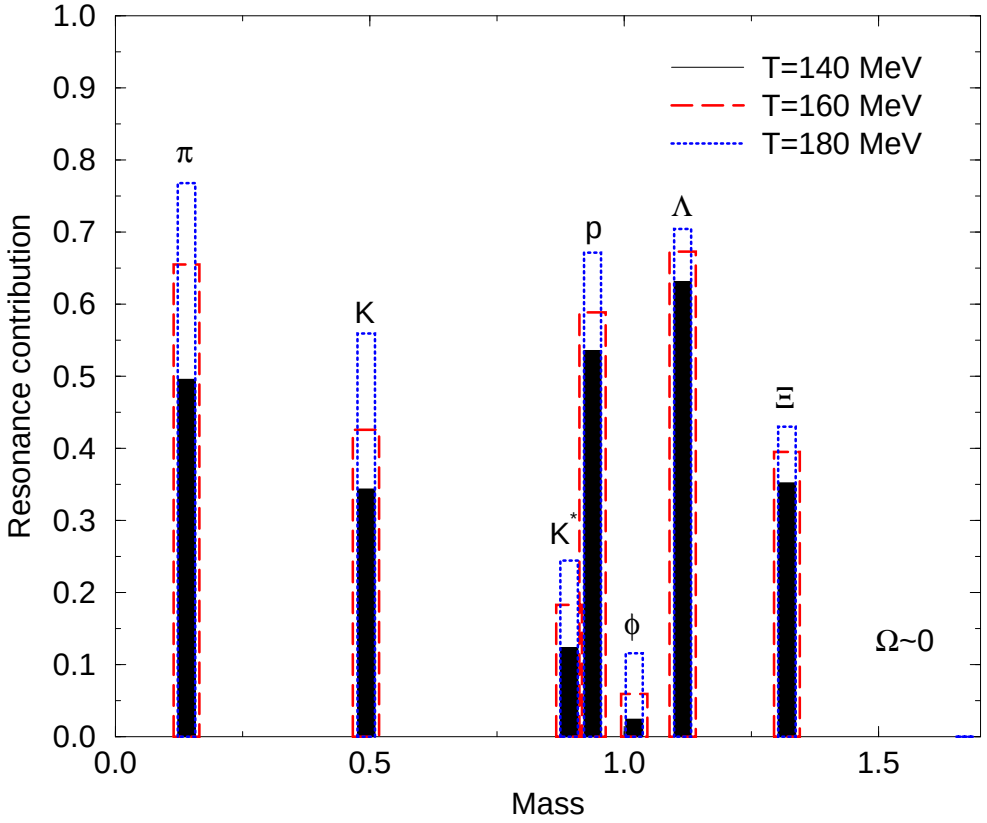

$$\frac{N^*}{N} = \frac{g^*(m^*T_{\rm H})^{3/2}e^{-m^*/T_{\rm H}}}{g(mT_{\rm H})^{3/2}e^{-m/T_{\rm H}}}$$

Resonances decay rapidly into 'stable' hadrons and dominate the yield of most stable hadronic particles.

Resonance yields test statistical hadronization principles.

Resonances reconstructed by invariant mass; important to consider potential for loss of observability.

HADRONIZATION GLOBAL FIT:→

OBSERVABLE RESONANCE YIELDS

Invariant mass method: construct invariant mass from decay products:

$$M^2 = (\sqrt{m_a^2 + \vec{p}_a^2} + \sqrt{m_b^2 + \vec{p}_b^2} + \ldots)^2 - (\vec{p}_a + \vec{p}_b + \ldots)^2$$

If one of decay products rescatter the reconstruction not assured.

Strongly interacting matter essentially non-transparent. Simplest model: If resonance decays $N^* \to D + \ldots$ within matter, resonance can disappear from view. Model implementation:

$$\frac{dN^*}{dt} = -\Gamma N^* + R, \quad \frac{dD}{dt} = \Gamma N^*, \quad \frac{dN^*_{\rm rec}}{dt} = \Gamma N^* - D\sum_j \langle \sigma_{Dj} v_{Dj}\rangle \rho_j(t)$$

To obtain the observable resonance yield $N^*_{\rm rec}$ we integrate to the time $t = \tau$ spend by N^* in the opaque matter, and add the remainder from free space decay. Regeneration term $R \propto \langle \sigma_{Di}^{INEL} v_{Di}\rangle \rho_i$ negligible since production reactions very much weaker than total scattering.Hadronic matter acts as black cloud, practically all in matter decays cannot be reconstructed.

TWO resonance ratios combined

natural widths **spread $\Gamma_{\Sigma^*} = 150$ MeV**

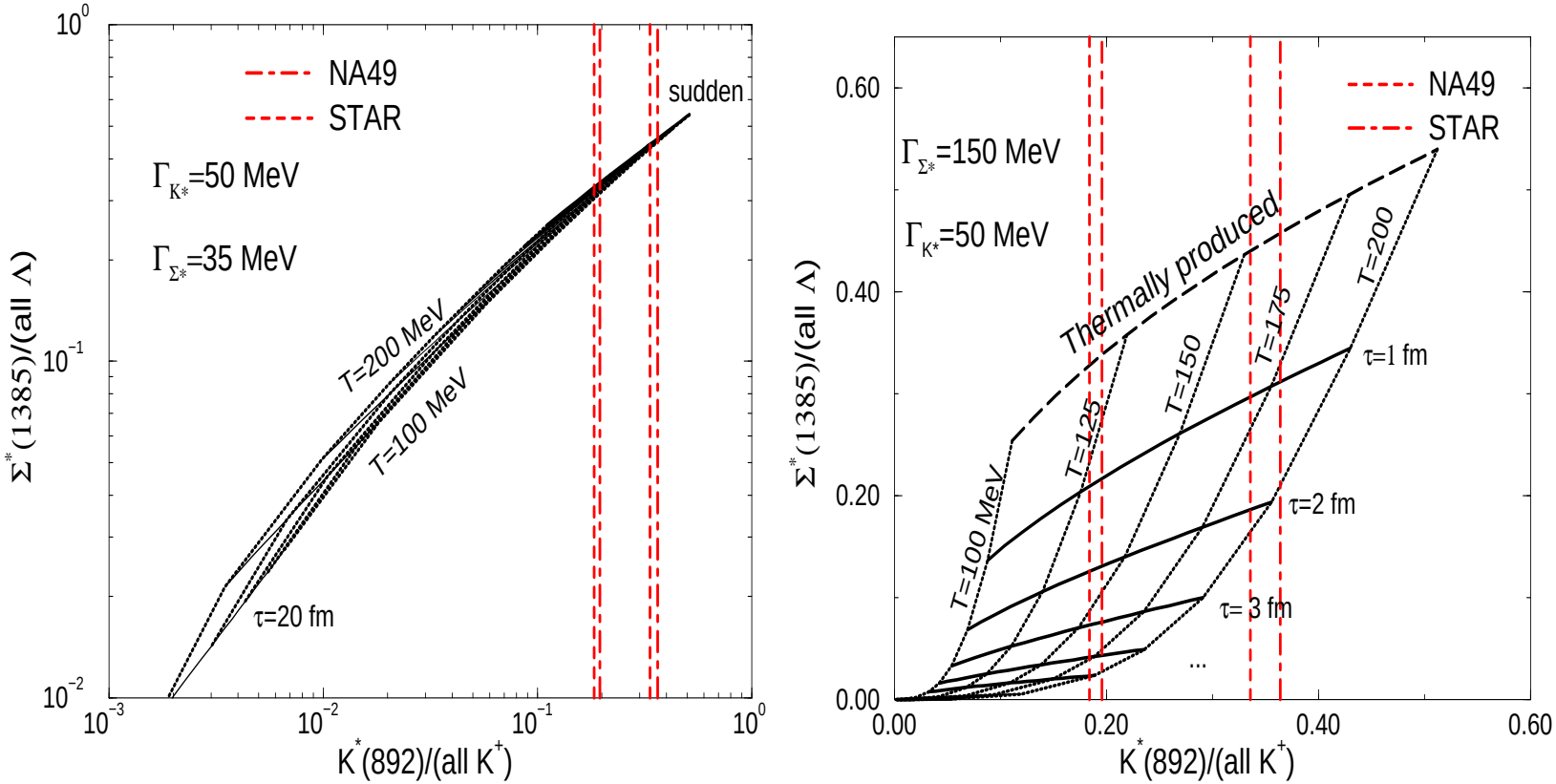

Dependence of the combined $\Sigma^*/(\text{all }\Lambda)$ with $K^*(892)/(\text{all K})$ signals on the chemical freeze-out temperature and HG phase lifetime.

Even the first rough measurement of K^*/K indicates that there is no long lived hadron phase. In matter widening makes this conclusion stronger.
Await forthcoming STAR Σ^* yields.

Statistical Hadronization fits of hadron yields

Full analysis of experimental hadron yield results requires a significant numerical effort in order to allow for resonances, particle widths, full decay trees, isospin multiplet sub-states.

Kraków-Tucson NATO supported collaboration produced a public package SHARE Statistical Hadronization with Resonances which is available e.g. at

http://www.physics.arizona.edu/~torrieri/SHARE/share.html

Lead author: Giorgio Torrieri

With W. Broniowski, W. Florkowski, J. Letessier, S. Steinke, JR nucl–th/0404083 Comp. Phys. Com. 167, 229 (2005)

Online SHARE: Steve Steinke No fitting online (server too small)

http://www.physics.arizona.edu/~steinke/shareonline.html

Aside of particle yields, also PHYSICAL PROPERTIES of the source are available, both in SHARE and ONLINE.

Centrality dependence at RHIC-200

DATA: Centrality dependence of dN/dy for $\pi^{\pm}$, $K^{\pm}$, p and $\bar{p}$. The errors are systematic only. The statistical errors are negligible. PHENIX data

N_{part}	π^+	π^-	K^+	K^-	p	$\bar{p}$
351.4	286.4 ± 24.2	281.8 ± 22.8	48.9 ± 6.3	45.7 ± 5.2	18.4 ± 2.6	13.5 ± 1.8
299.0	239.6 ± 20.5	238.9 ± 19.8	40.1 ± 5.1	37.8 ± 4.3	15.3 ± 2.1	11.4 ± 1.5
253.9	204.6 ± 18.0	198.2 ± 16.7	33.7 ± 4.3	31.1 ± 3.5	12.8 ± 1.8	9.5 ± 1.3
215.3	173.8 ± 15.6	167.4 ± 14.4	27.9 ± 3.6	25.8 ± 2.9	10.6 ± 1.5	7.9 ± 1.1
166.6	130.3 ± 12.4	127.3 ± 11.6	20.6 ± 2.6	19.1 ± 2.2	8.1 ± 1.1	5.9 ± 0.8
114.2	87.0 ± 8.6	84.4 ± 8.0	13.2 ± 1.7	12.3 ± 1.4	5.3 ± 0.7	3.9 ± 0.5
74.4	54.9 ± 5.6	52.9 ± 5.2	8.0 ± 0.8	7.4 ± 0.6	3.2 ± 0.5	2.4 ± 0.3
45.5	32.4 ± 3.4	31.3 ± 3.1	4.5 ± 0.4	4.1 ± 0.4	1.8 ± 0.3	1.4 ± 0.2
25.7	17.0 ± 1.8	16.3 ± 1.6	2.2 ± 0.2	2.0 ± 0.1	0.93 ± 0.15	0.71 ± 0.12
13.4	7.9 ± 0.8	7.7 ± 0.7	0.89 ± 0.09	0.88 ± 0.09	0.40 ± 0.07	0.29 ± 0.05
6.3	4.0 ± 0.4	3.9 ± 0.3	0.44 ± 0.04	0.42 ± 0.04	0.21 ± 0.04	0.15 ± 0.02

Include ϕ/K and K^*/K in fit (Star results)

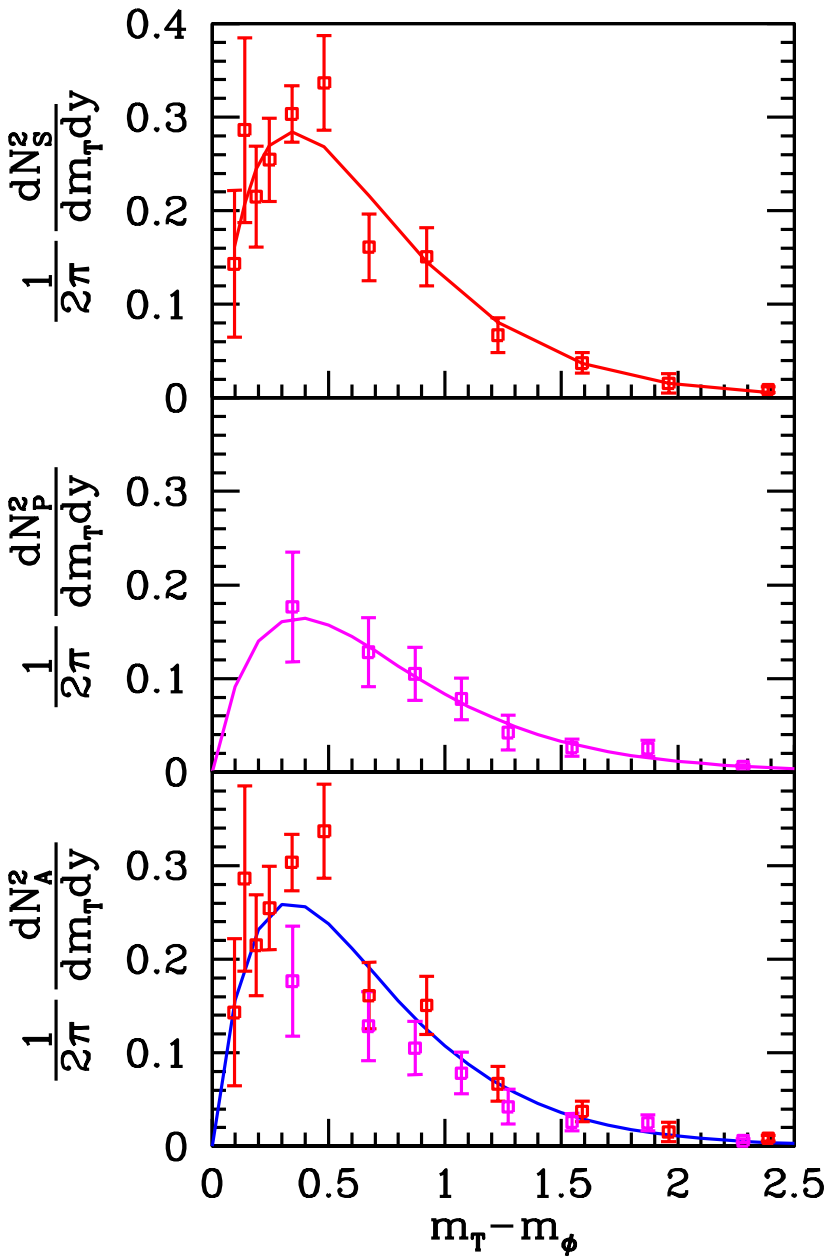

Include STAR data on $K^*(892)/K^-$, and ϕ/K^- relative yields, these help decisively fix γ_s ($\phi \propto \gamma_s^2$) and $T : Y \propto m^{3/2} e^{-m/T}$ for $m >> T$.

We considered the difference between STAR and PHENIX ϕ yields. The lines show our best fit results to STAR (top panel), PHENIX (middle panel) and combined data set (bottom panel). The integrated yields agree for the top two panels with those reported by the experimental collaborations. We note that the integrated yield derived from the combined data fit (bottom panel), to all available 10% centrality ϕ-yields, is not compatible with the PHENIX yield. This is so, since the evaluation of the integrated PHENIX ϕ-yield depends on the lowest $m_\perp$ measured yield. This data point appears to be a 1.5 s.d. low anomaly compared to the many STAR ϕ-results available at low $m_\perp$. This possibly statistical fluctuation materially influences the total integrated PHENIX ϕ-yield.

s/b and s/S rise with increasing centrality $A \propto V$; E/s falls

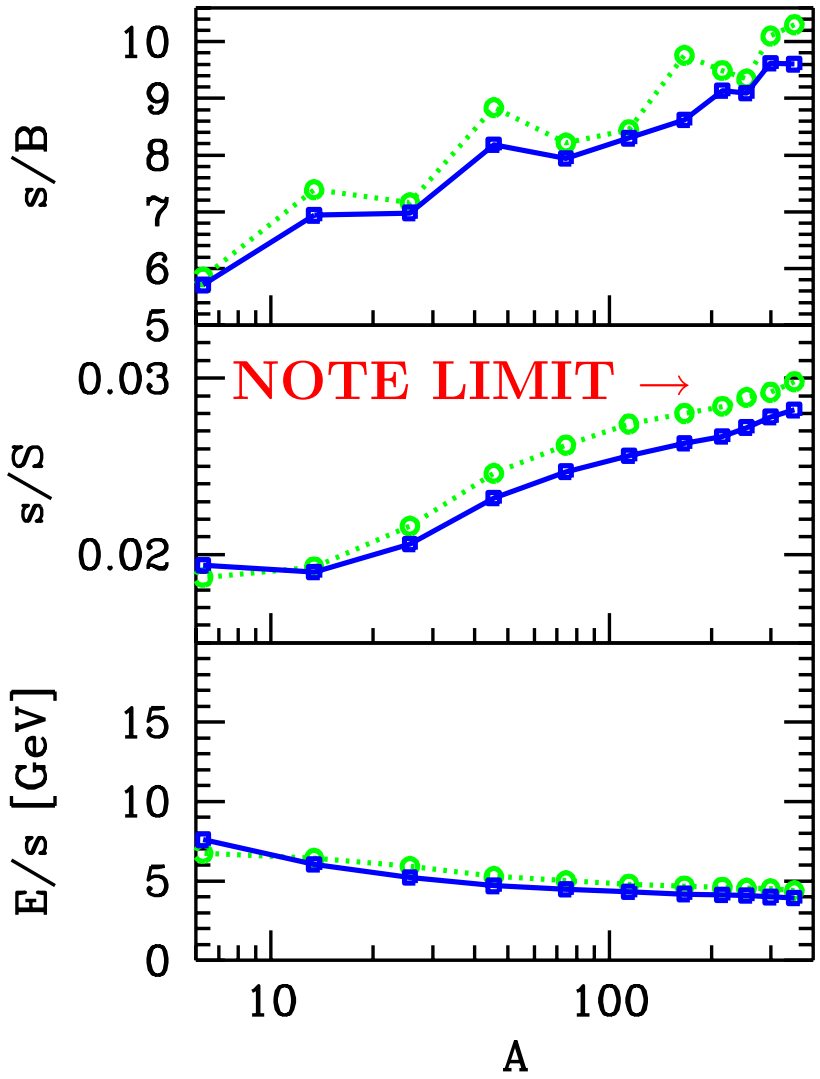

Showing results for both $\gamma_q, \gamma_s \neq 1$, for $\gamma_s \neq 1, \gamma_q = 1$. Note little difference in the result, even though the value of T will differ significantly.

1) $s/S \to 0.027$**, as function of** V**;**
2) most central value near QGP chemical equilibrium;
3) no saturation for largest volumes available;

Behavior is consistent with QGP prediction of steady increase of strangeness yield with increase of the volume, which implies longer lifespan and hence greater strangeness yield, both specific yield and larger $\gamma_s^{\rm QGP}$**.**

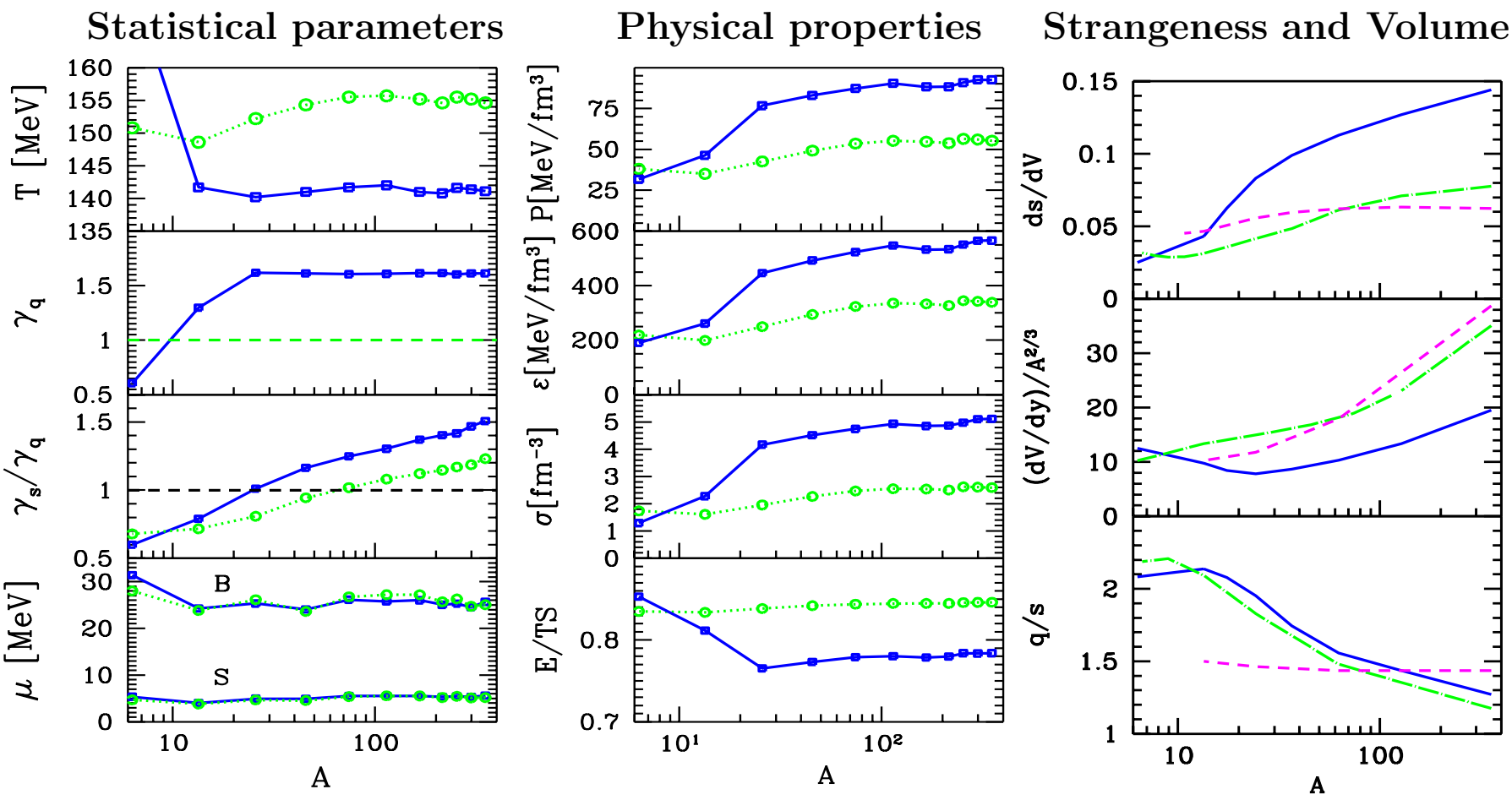

LINES: $\gamma_s, \gamma_q \neq 1$ **and** $\gamma_s \neq 1, \gamma_q = 1$, **also** $\gamma_s = \gamma_q = 1$

γ_q changes with $A \propto V$ from under-saturated to over-saturated value, $\gamma_s^{\rm HG}$ increases steadily to 2.4, implying near saturation in QGP. P, σ, ϵ increase by factor 2–3, at $A > 20$ (onset of new physics?), E/TS decreases with A.

Statistical + fit errors are seen in fluctuations, systematic error impacts absolute normalization by $\pm 10\%$.

RHIC200 PREDICTION OF dependence on centrality

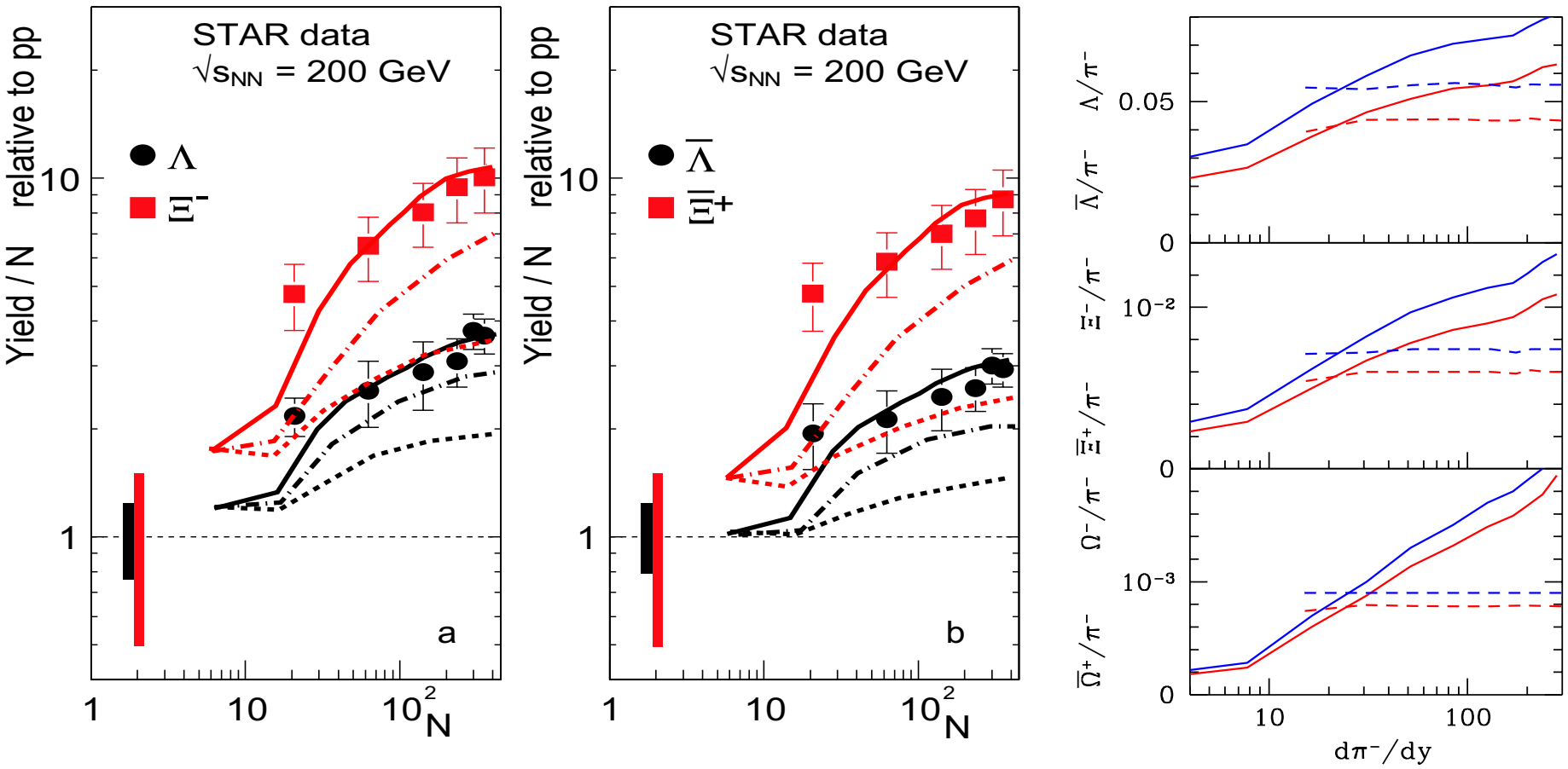

STAR $\sqrt{s_{\rm NN}} = 200$ GeV yields of hyperons $d\Lambda/dy$ and $d\Xi^-/dy$, (a), and anti-hyperons $d\overline{\Lambda}/dy$ and $d\overline{\Xi}^+/dy$, (b), normalized with, and as function of, A, relative to these yields in pp reactions: $d(\Lambda + \overline{\Lambda})/dy = 0.066 \pm 0.006$, $d(\Xi^- + \overline{\Xi}^+)/dy = 0.0036 \pm 0.0012$, $\overline{\Lambda}/\Lambda = 0.88 \pm 0.09$ and $\overline{\Xi}^+/\Xi^- = 0.90 \pm 0.09$. Solid lines, chemical non-equilibrium, dashed chemical equilibrium, (dash-dotted lines, semi-equilibrium.) On right, the predicted hyperons per π^- yields (blue for hyperons and for anti hyperons).

Particle yields as function of $\sqrt{s_{\rm NN}}$

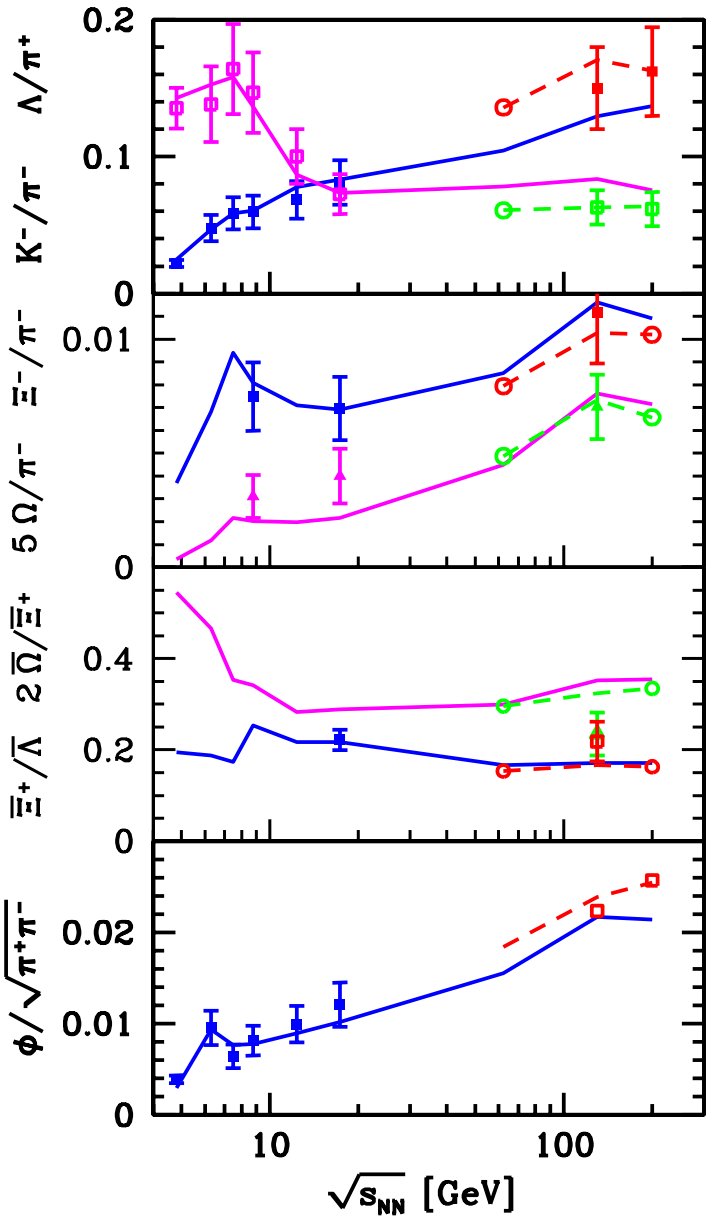

$\sqrt{s_{\rm NN}}$ [GeV]	$N_{4\pi}$ 5% 62.4	130	200	$dN/dy\|_{y=0}$ 5% 62.4	130	200
b	350.2	350.2	350.1	32.64	19.79	14.8
π^+	1001	1282	1470	225.8	236.6	237.4
π^-	1072	1368	1558	236.7	246.8	247.2
K^+	194.5	289.9	297.9	43.3	49.5	50.7
K^-	139.4	222.5	236.3	37,5	45.5	47.6
$\mathrm{K_S}$	162.3	248.2	259.2	39.2	45.9	47.5
ϕ	18.6	34.6	32.9	4.96	6.58	7.06
p	156.5	163.9	177.5	21.56	18.91	18.02
$\bar{p}.$	25.9	40.7	50.6	9.77	12.05	12.95
Λ	68.6	89.3	89.0	12.3	11.4	11.4
$\overline{\Lambda}$	16.0	29.1	32.2	5.91	7.94	8.7
Ξ^-	11.3	18.1	16.5	2.18	2.60	2.70
$\overline{\Xi}^+$	3.7	7.85	7.67	1.34	1.97	2.21
Ω	1.13	2.37	1.97	0.27	0.38	0.42
$\overline{\Omega}$	0.56	1.40	1.21	0.20	0.32	0.37
$\mathrm{K}^0(892)$	47.9	70.1	80.0	19.5	11.8	12.1
Δ^0	28.8	28.5	31.3	3.76	3.22	3.05
Δ^{++}	27.2	27.8	30.6	3.71	3.19	3.03
$\Lambda(1520)$	4.43	5.73	5.76	0.72	0.73	0.73
$\Sigma^+(1385)$	8.50	10.94	10.93	1.37	1.38	1.37
$\Xi 0(1530)$	2.98	4.90	4.45	0.59	0.71	0.74
η	110.2	158.7	172.7	26.3	29.6	30.3
η'	8.45	13.03	13.75	2.08	2.44	2.54
ρ^0	84.4	106	125	18.9	19.5	19.6
$\omega(782)$	75.5	94.9	112.2	17.1	17.6	17.6
$f_0(980)$	7.08	10.79	11.47	1.74	2.02	2.09

COMPARE $\sqrt{s_{\rm NN}}$ and V dependence of s/b and s/S, E/s

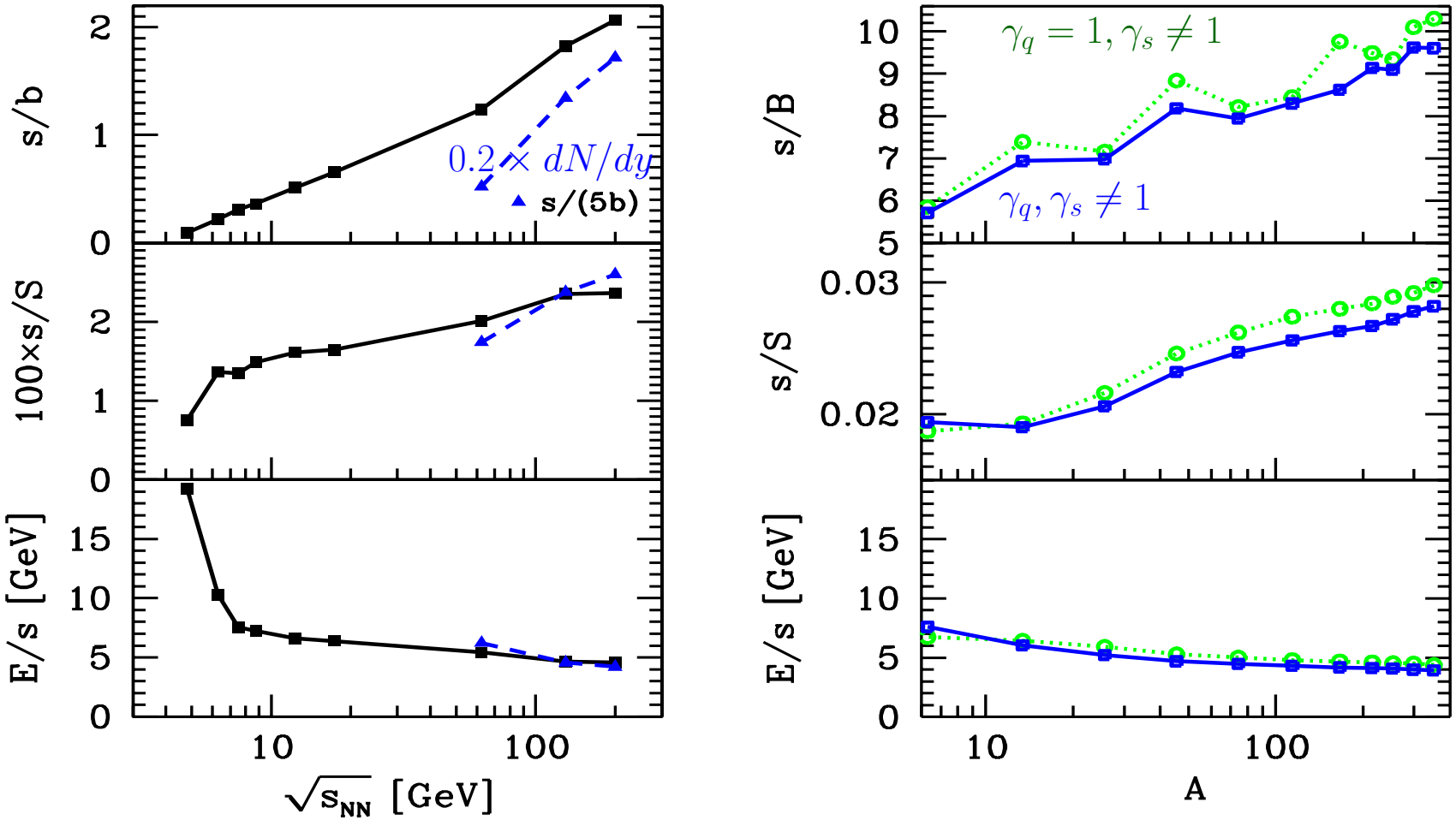

Full 4π and central rapidity results.
We again find $s/S \to 0.027$, as function of $\sqrt{s_{\rm NN}}$ and V: no saturation, consistent with QGP expectation and $\gamma_s^{\rm QGP} \simeq 1$, confirmed by s/B.
Energy/strangeness E/s cost drop at $\sqrt{s_{\rm NN}^{\rm cr}}$, suggests appearance of a new (e.g. $GG \to s\bar{s}$) production mechanism.

MOST SPECTACULAR

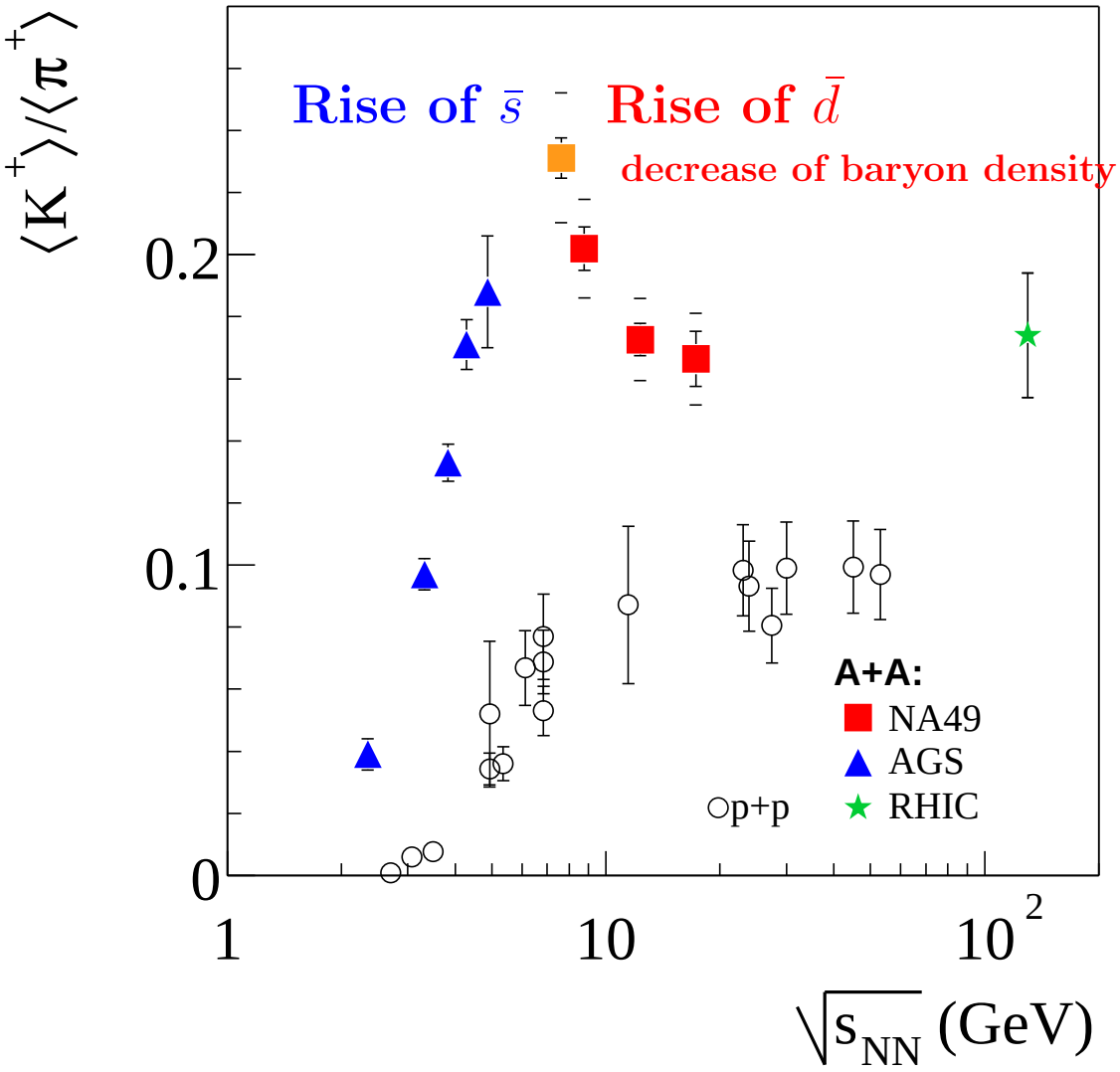

The NA49 (Marek Gaździcki) HORN

To describe the horn we need $\gamma_q \neq 1$

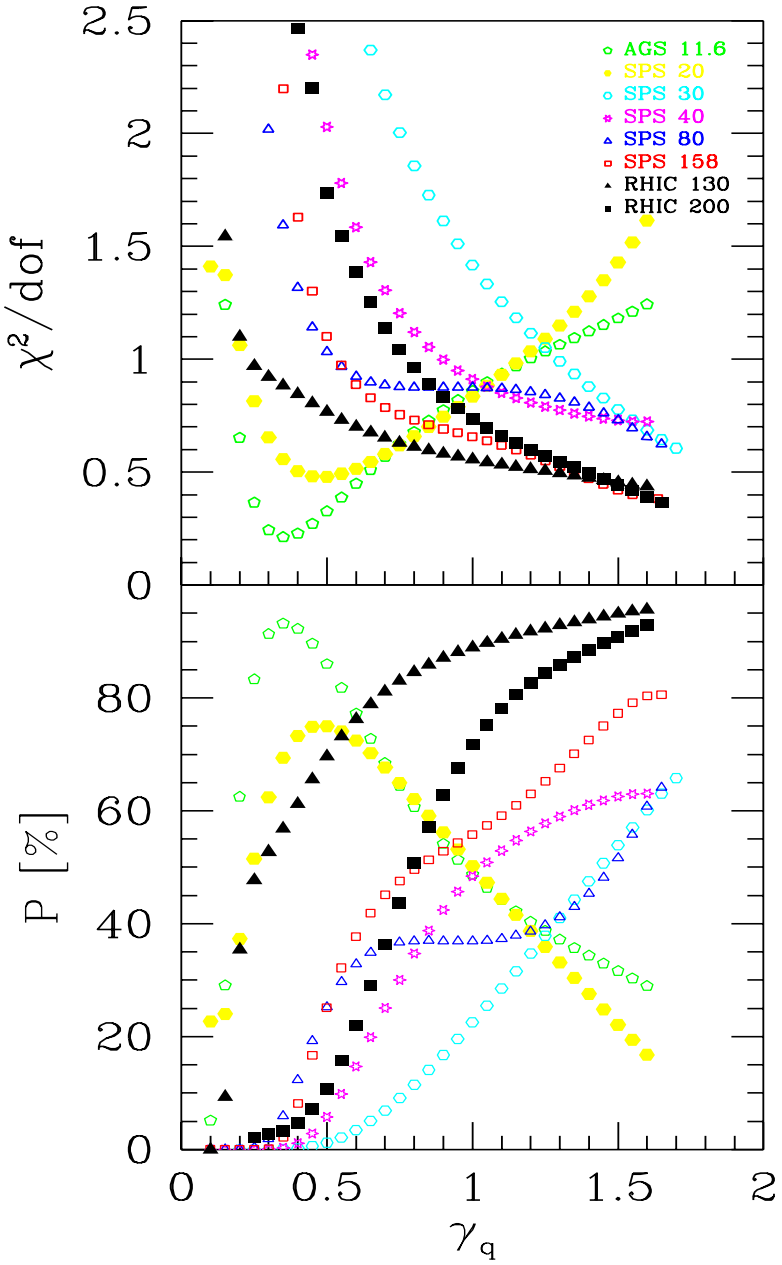

Looking a the fit χ^2 we see that between 20 and 30GeV results favor that γ_q jumps from highly unsaturated to fully saturated: from $\gamma_q < 0.5$ to $\gamma_q > 1.5$. This produces the horn (below). The individual fits relevant to understanding how the horn is created have good quality - see $P\%$.

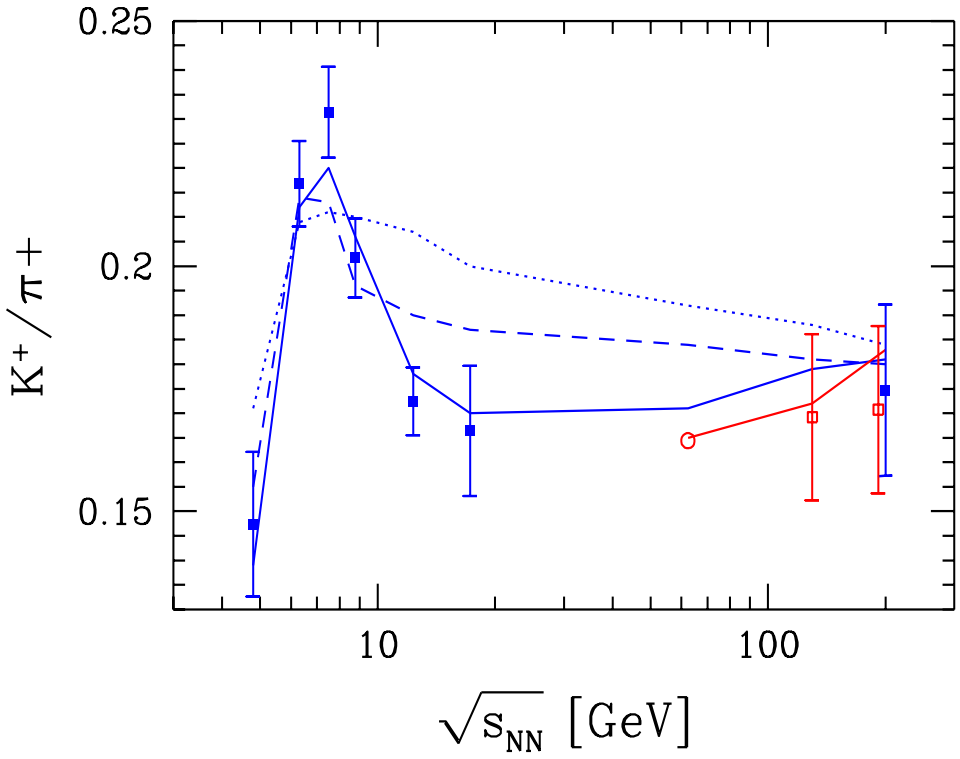

SUMMARY OF FIT RESULTS: Statistical parameters

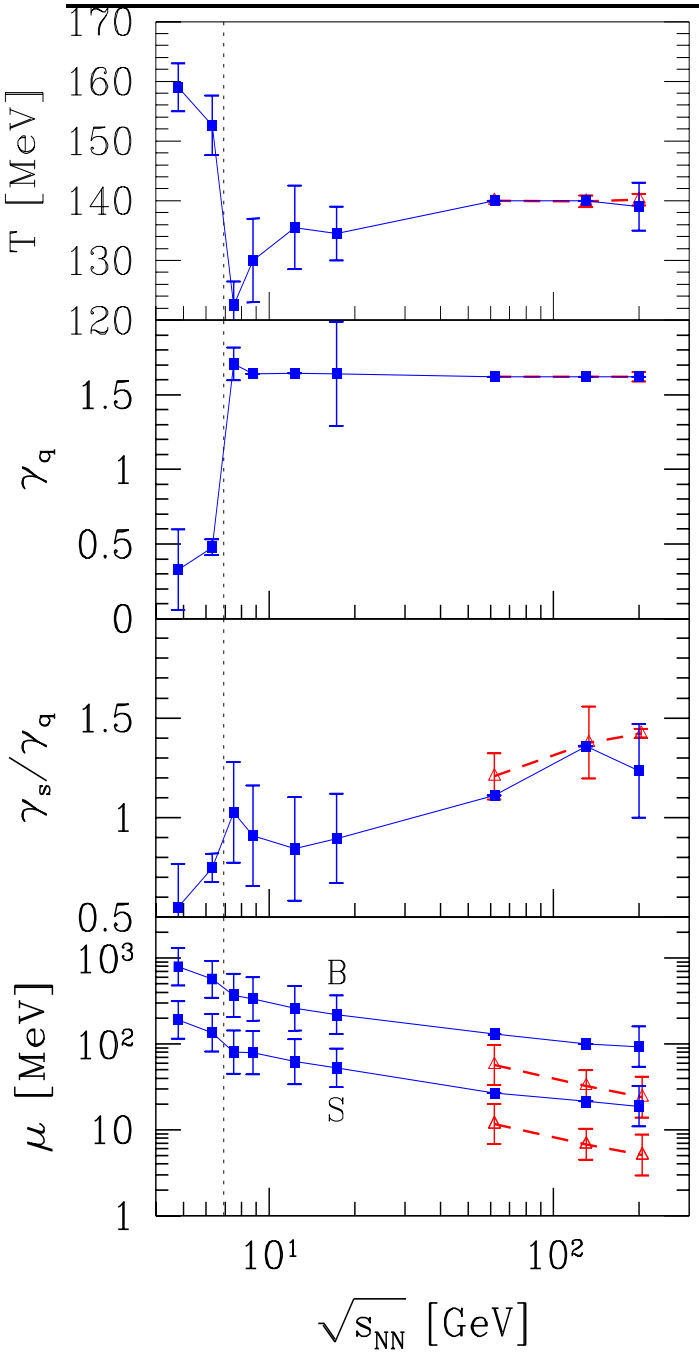

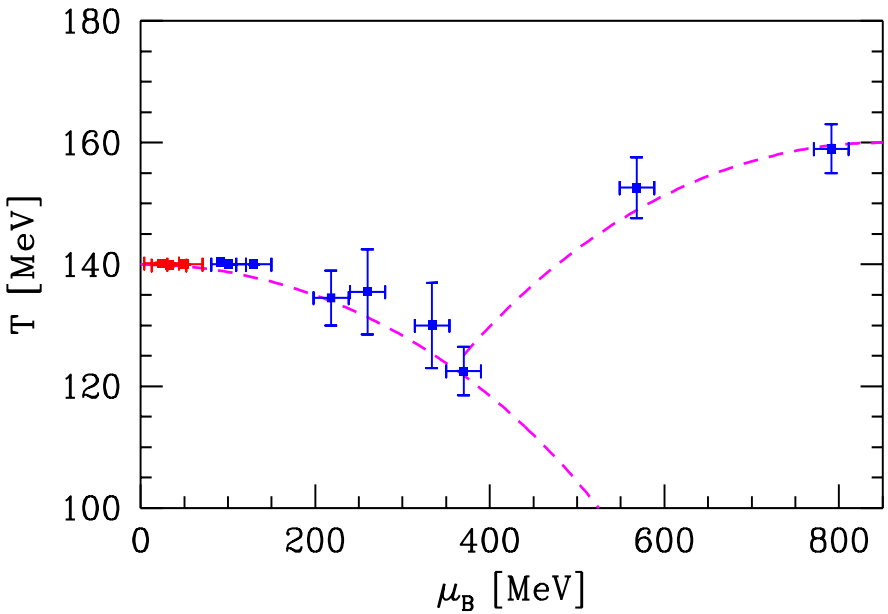

to be compared to, see below:

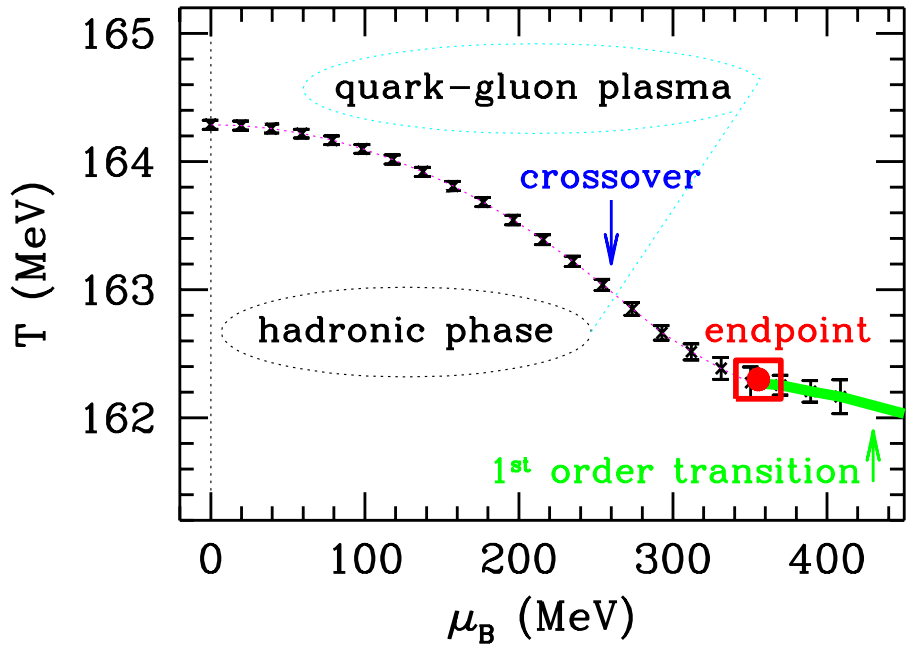

Why low/high PHASE BOUNDARY Temperature?

- **Dynamical effects of expansion:**
  colored partons like a wind, blow out the boundary
- **Degrees of freedom**
  - **Temperature of phase transition depends on available degrees of freedom.**
    For 2+1 flavors: $T = 162 \pm 3$, **for** $\gamma_s \to 0$
    $2 + 1 \to 2$ **flavor theory with** $T \to 170$ **MeV,**
    what happens when $\gamma_s \to 1.5$?
  - **The nature of phase transition/transformation changes when number of flavors rises from 2+1 to 3 is effect of** $\gamma_i > 1$ **creating a real phase transition?**
- **at high** $\mu_{\rm B}$ **we encounter**
  - **either conventional hadrons (contradiction with continuity of quark related variables: strangeness, strange antibaryons).**
  - **or more likely, a new heavy (valon) quark phases.**
    Under saturation of phase space compatible with higher T.

PHYSICAL PROPERTIES

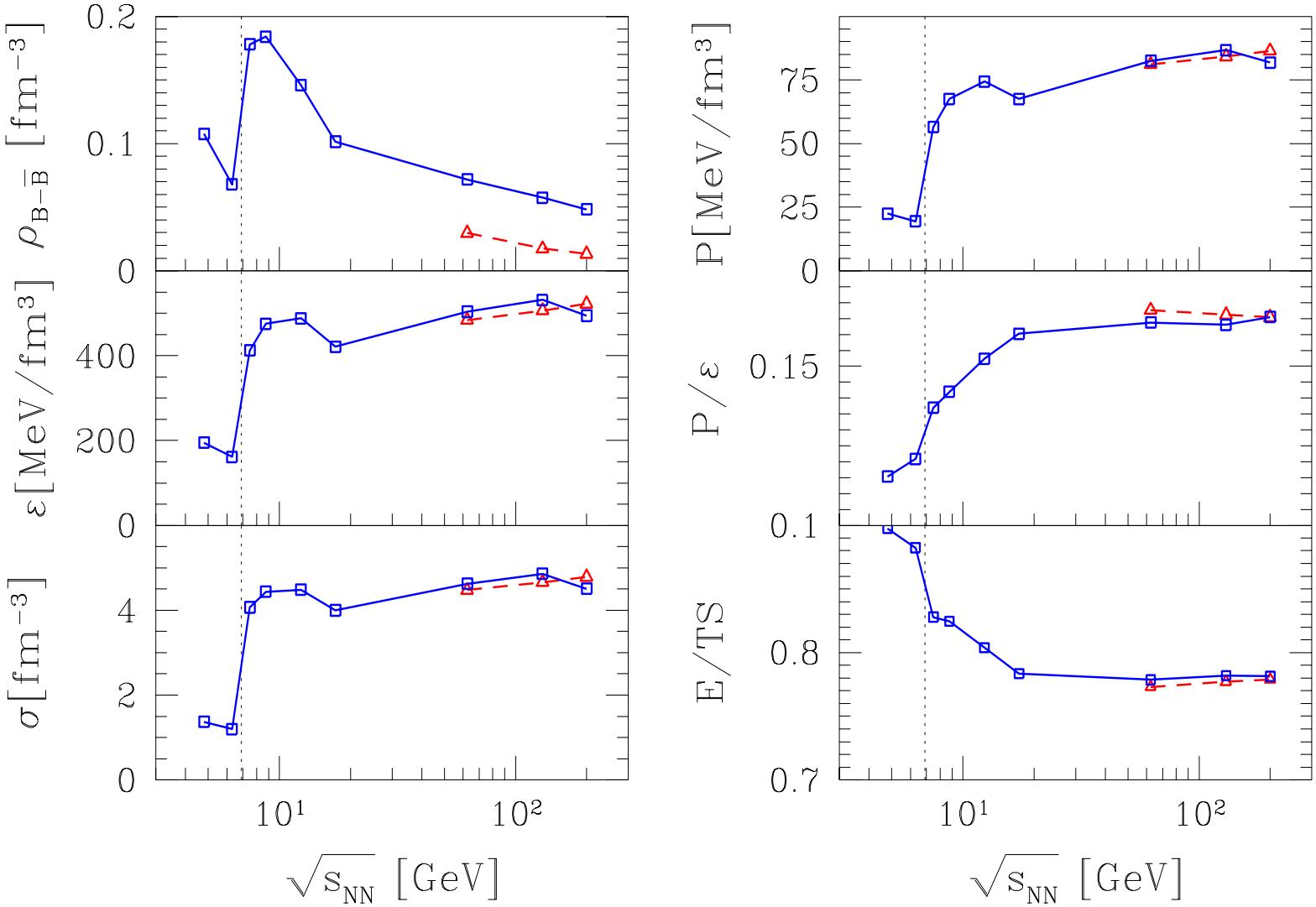

Note the large jumps by factor 2–3 in densities (to left) and pressure (on right) as the collision energy changes from 20 GeV to 30 GeV. There is clear evidence of change in reaction mechanism. There no difference between top SPS and RHIC energy range.

RHIC200 dependence on centrality=dependence on energy

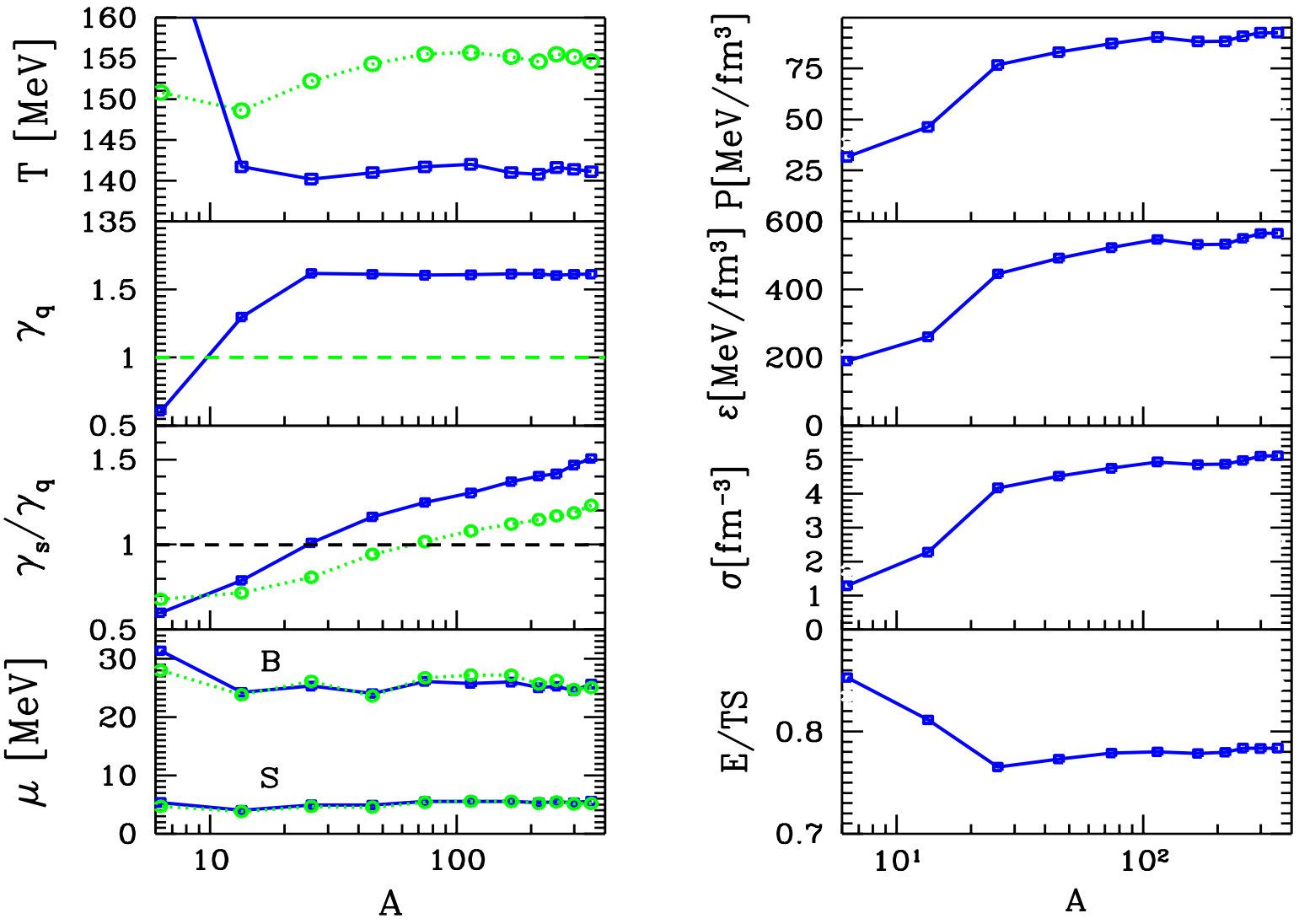

$\gamma_s \neq 1$ $\gamma_s, \gamma_q \neq 1$ **Note:** γ_q **moves from under-saturated to over-saturated value,** P, σ, ϵ **increase by factor 2–3,** E/TS **decreases, just as we saw it as function of** $\sqrt{s}$**.**
JR, J. Letessier and G. Torrieri, nucl-th/0412072

s/b and s/S rise with energy and centrality E/s falls

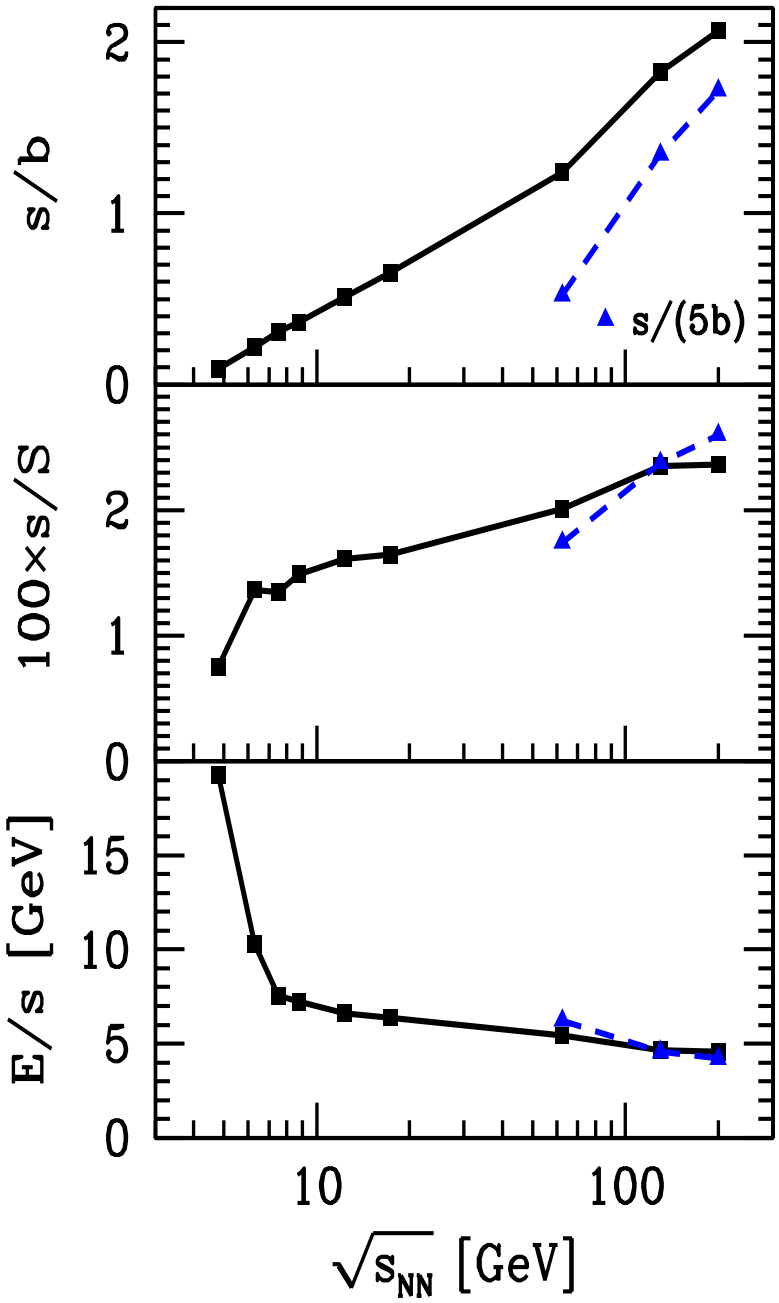

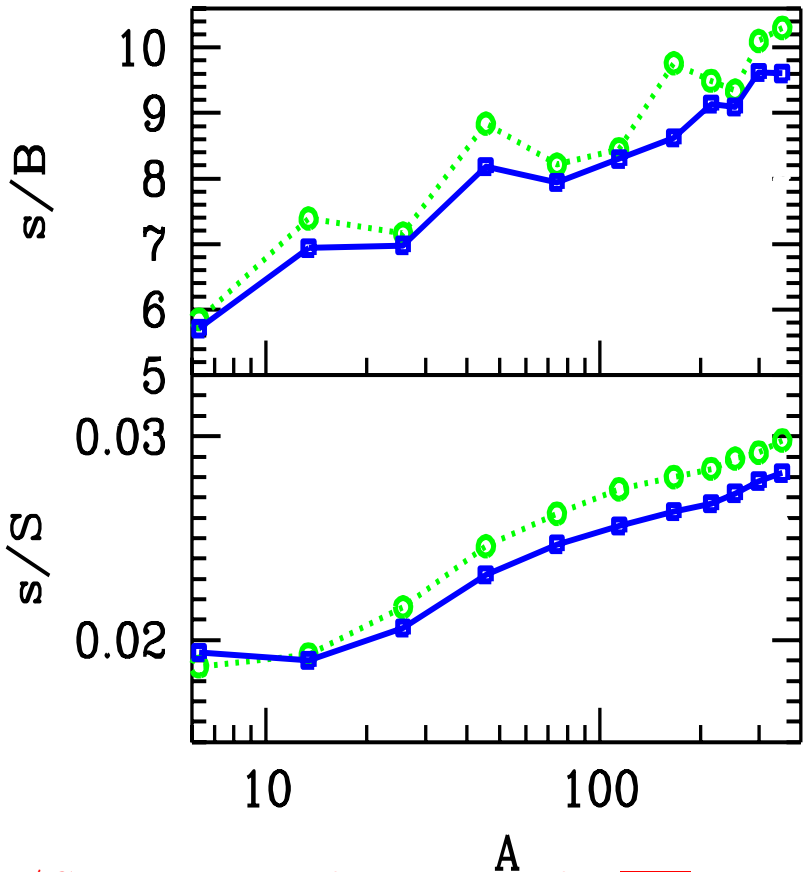

$s/S \to 0.027$ as function of $\sqrt{s_{\rm NN}}$ and V: **INITIAL QGP!**

Energy/strangeness breaks at $\sqrt{s^{\rm cr}_{\rm NN}}$
Different cost → different mechanism!

Excursion to Pentaquarks

Statistical hadronization allows to explore the rate of production of pentaquarks which depend on chemical potentials [PRC68, 061901 (2003), hep-ph/0310188]; $\Theta^+(1540)$ is best looked for at low reaction energy.

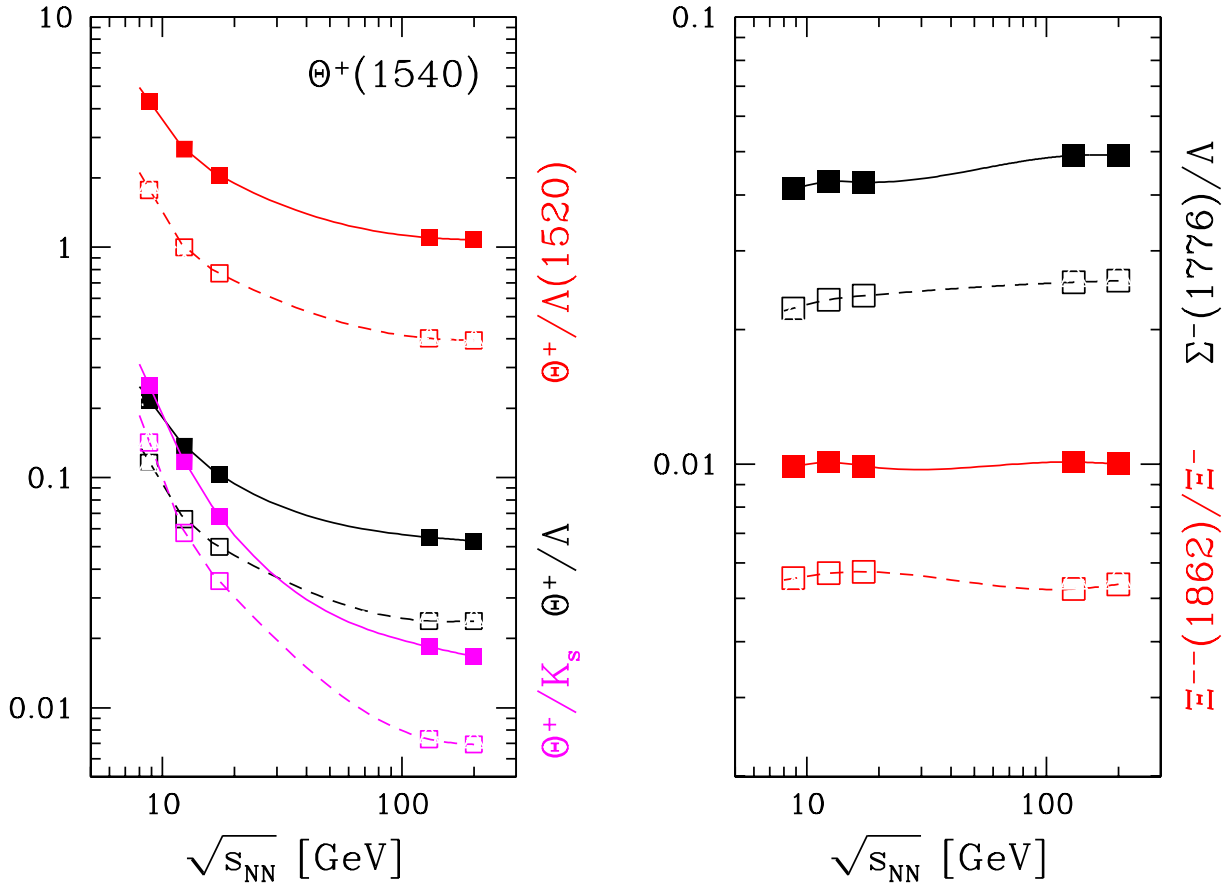

Expected relative yield of $\Theta^+(1540)$(left); $\Xi^{--}(1862)$ and $\Sigma^-(1776?)$ (right), based on statistical hadronization conditions at SPS and RHIC: solid lines γ_s and γ_q fitted; dashed lines γ_s fitted, $\gamma_q = 1$.

4. Particle yields expected at LHC

LHC

Assuming that statistical hadronization model applies, we have 7 parameters needing fixing:

1) $\mu_b \equiv T\ln(\lambda_u\lambda_d)^{3/2}$**, the baryon and**
2) $\mu_S \equiv T\ln[\lambda_q/\lambda_s]$**, hyperon chemical potentials;**
3) $\lambda_{I3} \equiv \lambda_u/\lambda_d$**, a fugacity distinguishing the up from the down quark flavor;**
4) γ_s **the strangeness phase space occupancy;**
5)γ_q **the light quark phase space occupancy;**
6) T**, the (chemical) freeze-out temperature;**
7) dV/dy**, the volume related a given rapidity to the particle yields;**

There are several constraints and physical conditions:

1) What is baryon stopping? use $dE/db = 412 \pm 20\,\mathrm{GeV}$, μ_b **is hard to measure .**
2) Strangeness conservation, we set $(\bar{s}-s)/(\bar{s}+s) = 0 \pm 0.01$**, this fixes** μ_S **given** μ_b**.**
3) The electrical charge to net baryon ratio, we set $Q/b = 0.39 \pm 0.01$**. Fixes** λ_{I3}
4-5) The value of γ_s^{h} **will be varied, the value of** γ_q^{h} **set either to unity (for equilibrium) or max allowed value 1.6–1.7.**
6) We rely on $E/TS \to 0.78$ **for non-equilibrium and** $\to 0.845$ **for equilibrium**
7) particle ratios limit need for volume normalization.

Range of Parameters / Physical Freeze-out Conditions at LHC

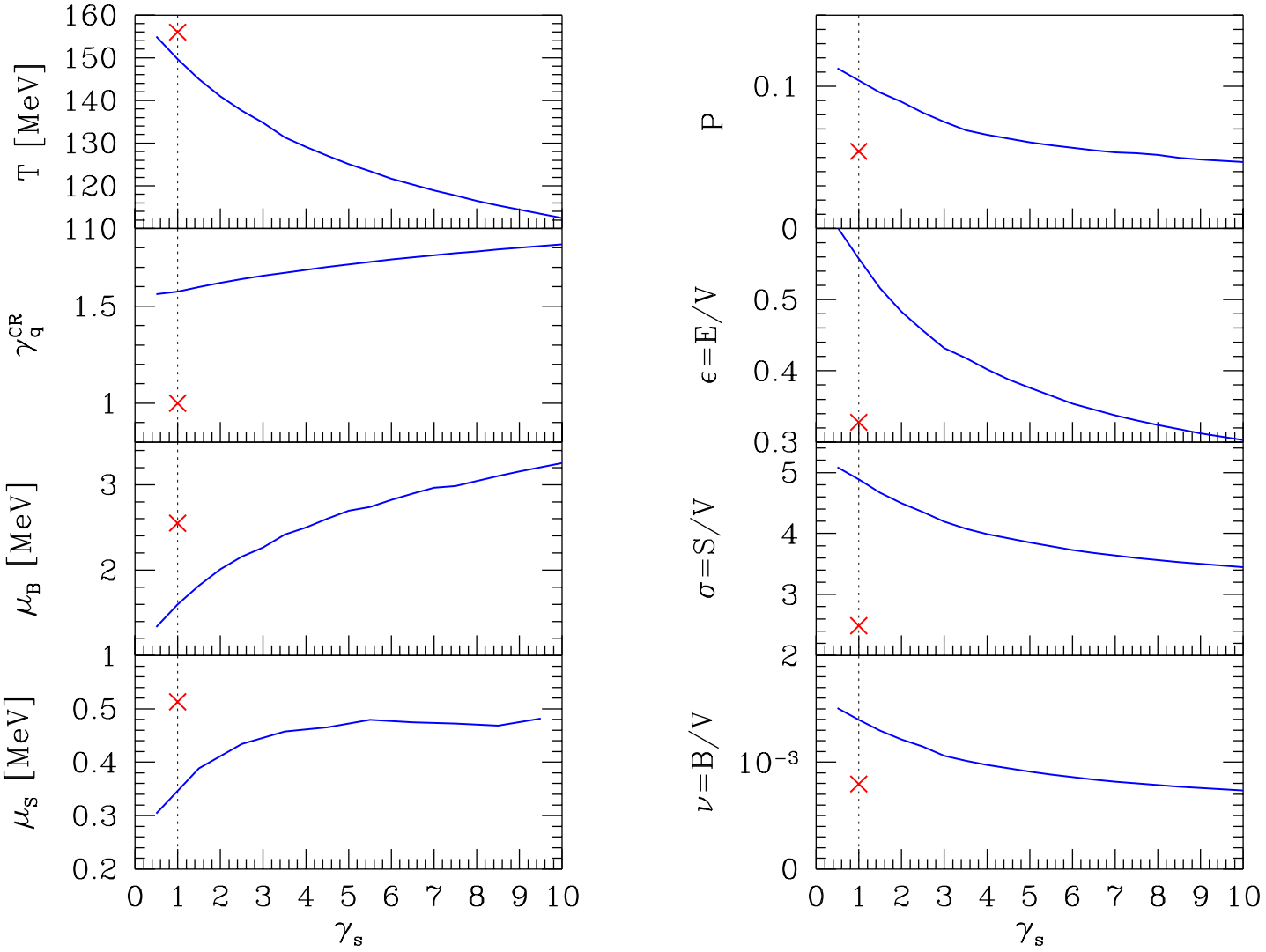

On left: The values of T, $\gamma_q^{\rm CR}$, $\mu_{\rm B}$, and $\mu_{\rm S}$ as function of varying γ_s, the equilibrium model results are crosses at $\gamma_s = 1$ for $\gamma_q = 1$.

On right : Pressure P [GeV/fm^3], energy density ϵ [GeV/fm^3], entropy density $\sigma = S/V$ [1/fm^3], net baryon density $\nu = (B - \overline{B})/V = b/V$ [1/fm^3], for non-equilibrium SHM. Cross at γ_s for chemical equilibrium.

Particle ratios at LHC

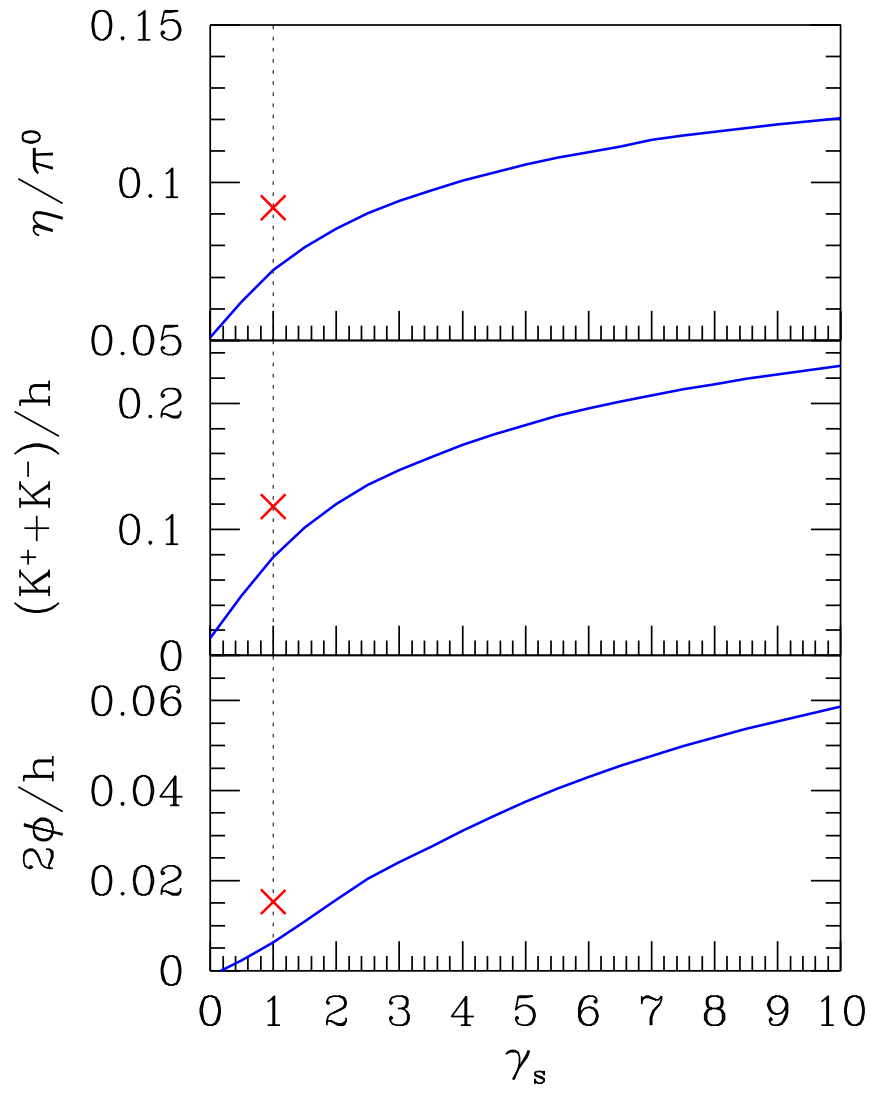

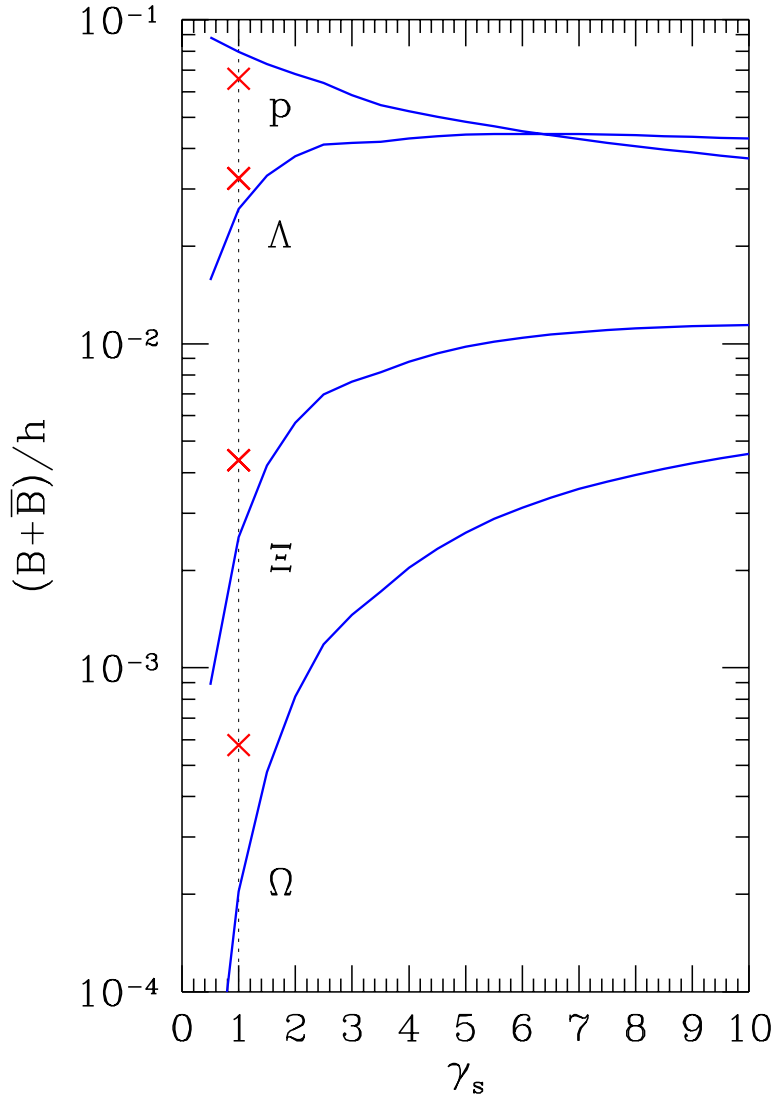

All yields after weak decay of hyperons and $\mathrm{K_{S,L}}$, crosses denote chemical equilibrium result. $h = h^+ + h^- \equiv p + \bar{p} + \pi^+ + \pi^- + \mathrm{K}^+ + \mathrm{K}^-$, **NEXT PAGE: all yields BEFORE weak decays.**

$dV/dy =$ $=3600$ fm^3 dN/dy	$T = 156$ $\gamma_s^{\rm H} = \gamma_q^{\rm H} = 1$ $\mu_{\rm B} = 2.57, \mu_{\rm S} = 0.51$	$T = 145$ $\gamma_s^{\rm H} = \gamma_q^{\rm H} = 1.62$ $\mu_{\rm B} = 1.83, \mu_{\rm S} = 0.40$	$T = 135$ $\gamma_s^{\rm H} = 3, \gamma_q^{\rm H} = 1.67$ $\mu_{\rm B} = 2.28, \mu_{\rm S} = 0.45$	$T = 125$ $\gamma_s^{\rm H} = 5, \gamma_q^{\rm H} = 1.73$ $\mu_{\rm B} = 2.70, \mu_{\rm S} = 0.48$
s/S	**0.025**	**0.021**	**0.029**	**0.034**
π^+	**466.22**	**866.24**	**655.12**	**506.6**
π^-	**480.48**	**889.48**	**682.24**	**535.6**
π^0	**524.98**	**966.74**	**751.16**	**598.4**
K^+	**84.60**	**137.62**	**163.48**	**176.9**
K^-	**84.16**	**136.98**	**162.54**	**175.8**
$\mathrm{K_S}$	**81.96**	**133.42**	**156.82**	**168.1**
ϕ	**10.95**	**15.73**	**26.86**	**36.54**
p	**32.80**	**64.98**	**36.12**	**19.98**
$\bar{p}$	**31.76**	**63.42**	**34.96**	**19.18**
Λ	**16.76**	**32.24**	**28.34**	**21.9**
$\overline{\Lambda}$	**16.33**	**31.62**	**27.58**	**21.1**
Ξ^-	**3.12**	**5.94**	**8.46**	**9.46**
$\overline{\Xi}^+$	**3.06**	**5.86**	**8.28**	**9.20**
Ω	**0.416**	**0.724**	**1.634**	**2.56**
$\overline{\Omega}$	**0.410**	**0.718**	**1.610**	**2.52**
$\mathrm{K}^0(892)$	**24.78**	**35.58**	**35.34**	**31.2**
$\Delta^0 = \Delta^{++}$	**6.16**	**11.66**	**5.68**	**2.70**
$\Lambda(1520)$	**1.29**	**2.220**	**1.66**	**1.08**
$\Sigma^-(1385)$	**2.14**	**3.98**	**3.28**	**2.34**
$\Xi^0(1530)$	**0.914**	**1.656**	**2.26**	**2.46**
η	**59.6**	**95.2**	**93.4**	**90.2**
η'	**5.32**	**7.62**	**7.78**	**7.06**
ρ^0	**53.8**	**79.2**	**48.4**	**29.8**
$\omega(782)$	**49.8**	**72.2**	**42.4**	**25.0**
$f_0(980)$	**4.50**	**6.42**	**6.28**	**5.44**

7. Conclusions

- **Experimental data imply fast hadronization without re-equilibration;**
- **This allows us to study the QGP fireball at the end of its evolution by considering hadron production within here presented statistical hadronization analysis;**
- **A–A reactions at top SPS and at RHIC energies are different from p–p and AGS A–A which seem to satisfy string fragmentation and hadron thermalization dynamics.**
- **LHC will help complete the understanding of QGP hadronization**
- **Dynamical hadronization model next step. Will lead to full understanding of hadron production including particle spectra.**